CHALMERS
UNIVERSITY OF TECHNOLOGY

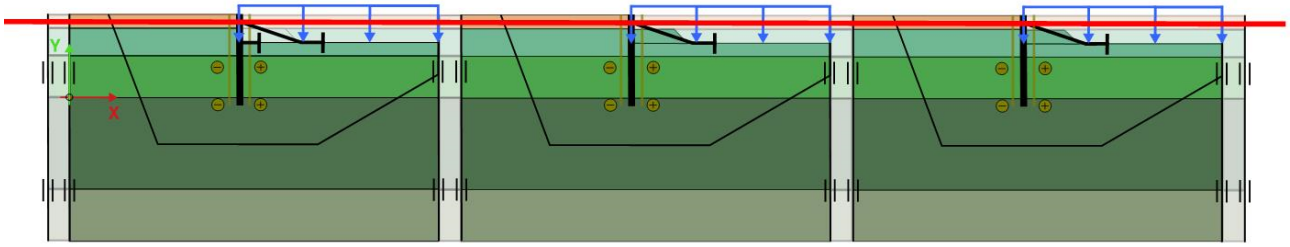

Numerical Modelling of a Staged Excavation in Soft Clay

A case study of the Tennet 2 project

Master's Thesis in the Master's Programme Infrastructure and Environmental Engineering

LARS FAGERGREN
BALTZAR LINDE

Department of Civil and Environmental Engineering
Division of GeoEngineering
Geotechnical Engineering Research Group
CHALMERS UNIVERSITY OF TECHNOLOGY
Master's Thesis BOMX02-17-29
Gothenburg, Sweden 2017

MASTER'S THESIS BOMX02-17-29

Numerical Modelling of a Staged Excavation in Soft Clay

A case study of the Tennet 2 project

Master's Thesis in the Master's Programme Infrastructure and Environmental Engineering

LARS FAGERGREN

BALTZAR LINDE

Department of Civil and Environmental Engineering
Division of GeoEngineering
Geotechnical Engineering Research Group
CHALMERS UNIVERSITY OF TECHNOLOGY

Göteborg, Sweden 2017

Numerical Modelling of a Staged Excavation in Soft Clay
A case study of the Tennet 2 project

Master's Thesis in the Master's Programme Infrastructure and Environmental Engineering

LARS FAGERGREN

BALTZAR LINDE

Examensarbete BOMX02-17-29/ Institutionen för bygg- och miljöteknik,
Chalmers tekniska högskola 2017

Department of Civil and Environmental Engineering
Division of GeoEngineering
Geotechnical Engineering Research Group
Chalmers University of Technology
SE-412 96 Göteborg
Sweden
Telephone: + 46 (0)31-772 1000

Cover:
Setup of three of the modelled cross-sections in the staged excavation.

Chalmers Reproservice. Göteborg, Sweden, 2017

Numerical Modelling of a Staged Excavation in Soft Clay
A case study of the Tennet 2 project

Master's thesis in the Master's Programme Infrastructure and Environmental Engineering

LARS FAGERGREN
BALTZAR LINDE
Department of Civil and Environmental Engineering
Division of GeoEngineering
Geotechnical Engineering Research Group
Chalmers University of Technology

ABSTRACT

In soft clay, excavations normally need to be supported by retaining walls. In order to minimize the need of other structural support and to reduce structural movements, the method of staged excavation is commonly used. To ensure that requirements regarding safety and displacements are fulfilled, numerical modelling is commonly used.

Numerical modelling can be performed in both two and three dimensions, and the evaluation of excavations is in reality a three dimensional problem. This causes the calculations to be quite complex and time consuming. In order to decrease the computational time, the modelling could be done in two dimensions instead. However, two-dimensional models are often based on conservative assumptions that could potentially result in additional construction costs.

This thesis aimed to evaluate the potential of using a 2.5-dimensional model in the finite element analysis software PLAXIS 2D. The intention of this model was to simulate three-dimensional conditions of a staged excavation, by using a two-dimensional setup. The model was validated by comparing the generated results to measured deformations at the project Tennet 2 by Skanska Sverige AB. Furthermore, by comparing two constitutive models, it was possible to investigate which of the models that simulated the conditions in the most reliable way. These models were the Mohr-Coulomb and Soft Soil model.

The setup of the 2.5D-model was found to be challenging due to the uncertainties regarding soil parameters and simplifications of the structure. As a result of this, it was difficult to further conclude which constitutive model that was the most suitable. However, it could be stated that the consolidation analysis with the Mohr-Coulomb model, using the drainage type Undrained (A), simulated the most accurate deformations close to the surface. Consolidation analysis with the Soft Soil model, using Undrained (A) with the low values of the modified swelling index, κ^*, simulated better the deformations at greater depth. The most noticeable drawback, with the setup of the 2.5D-model, was the fact that the positive contribution of the surrounding soil was not fully utilised. If this was to be improved, the simulated deformations would reflect the measured deformations in a more accurate way.

Key words: 2.5D-Model, Deformations, Finite element method, Geotechnics, Lateral earth pressure, Mohr-Coulomb, Numerical modelling, PLAXIS 2D, Sheet pile wall, Soft Soil, Staged excavation, Stiffness, Wailing beam

Numerisk modellering av etappvis schakt i lös lera
En fallstudie av projektet Tennet 2

Examensarbete inom masterprogrammet Infrastucture and Environmental Engineering

LARS FAGERGREN
BALTZAR LINDE
Institutionen för bygg- och miljöteknik
Avdelningen för geologi och geoteknik
Forskargruppen för geoteknik
Chalmers tekniska högskola

SAMMANFATTNING

I lös lera behövs schakter ofta stödjas upp av sponter. För att minimera behovet av andra stödkonstruktioner och för att minska rörelser i samband med schakten används ofta metoden med etappvis schakt. För att säkerställa att kraven på säkerhet och rörelser är uppfyllda utnyttjas vanligtvis numerisk modellering.

Numerisk modellering kan utföras i både två och tre dimensioner, och utvärderingen av schakter är i realiteten ett tredimensionellt problem. Detta gör att beräkningarna blir relativt komplexa och tidskrävande. För att istället minska beräkningstiden kan modelleringen utföras i två dimensioner. Tvådimensionella beräkningar är dock ofta baserade på konservativa antaganden som kan resultera i ökade konstruktionskostnader.

Avsikten med denna rapport är att utvärdera möjligheten att använda en 2.5-dimensionell modell i det finita element programmet PLAXIS 2D. Intentionen med modellen var att simulera tredimensionella förhållanden genom att använda en tvådimensionell struktur. Modellen validerades genom att jämföra de genererade resultaten med uppmätta deformationer från projektet Tennet 2 utfört av Skanska Sverige AB. Genom att jämföra två olika konstitutiva modeller var det möjligt att undersöka vilken som återskapade förhållandena bäst. Dessa två modeller var Mohr-Coulomb- och Soft Soil-modellen.

Det visade sig vara utmanande att konstruera 2.5D-modellen då det fanns osäkerheter gällande jordparametrar och förenklingar av strukturen. Detta ledde till att det var svårt att fastställa vilken konstitutiv modell som var mest lämplig. Det kan dock konstateras att konsolideringsanalys med Mohr-Coulomb-modellen, med dräneringstypen Undrained (A), simulerade deformationerna vid ytan bäst. Konsolideringsanalys med Soft Soil-modellen, med Undrained (A) och de låga värdena på det modifierade svällningsindexet, κ^* , återskapade deformationerna bättre på djupet. Den mest uppenbara bristen med 2.5D-modellen var det faktum att stabiliteten från den omgivande jorden inte utnyttjades till fullo. Vid förbättring av detta skulle de simulerade deformationerna bättre återspegla dem uppmätta.

Nyckelord: 2.5D-model, Deformationer, Etappvis schakt, Finita element metoden, Geoteknik, Hammarband, Mohr-Coulomb, Numerisk modellering, PLAXIS 2D, Sidojordtryck, Soft Soil, Spont, Styvhet

Contents

Preface

This thesis has been carried out during the spring 2017 at the Department of Infrastructure and Environmental Engineering at Chalmers University of Technology in collaboration with Skanska Teknik and Skanska Grundläggning. The idea behind the thesis was initiated by Skanska but has been modified many times during the months of progress.

First, we would like to thank our supervisor at Skanska Teknik, Ph.D Anders Kullingsjö, for the great support and interest when the time was short. We are also very grateful for the guidance given from Ph.D Torbjörn Edstam, Cecilia Edmark and the staff at Skanska Teknik. The many hints have been essential when we got lost in the jungle of geotechnics. Many thanks also to our supervisor at Chalmers, Minna Karstunen, for the useful information provided throughout the project.

The thesis writing would have been dull if it was not for the company and the supportive conversations throughout the process with Caroline Björk Tocaj and Erik Toller. Best of luck in the future.

Finally, and above all, we would like to express our sincere gratitude to our families and friends who have endured our company during the many years of study.

Göteborg June 2017

Lars Fagergren and Baltzar Linde

Notations

Roman upper case letters

E	Young's modulus
E'	Effective Young's modulus
E_{ur}	Unloading/reloading modulus
EA	Normal stiffness
EI	Flexural rigidity
K_0	Lateral earth pressure coefficient at rest
$K_{0,NC}$	Lateral earth pressure coefficient at rest for normally consolidated soil
K_a	Active earth pressure coefficient
K_p	Passive earth pressure coefficient
L	Length spacing
M	Critical failure line
M_0	Constant constrained modulus below effective vertical preconsolidation pressure
M_L	Constant constrained modulus between vertical preconsolidation pressure and the limit stress
M_{ur}	Constant constrained modulus at unloading/reloading
R	Interface parameter
R_{inter}	Interface value (PLAXIS 2D)

Roman lower case letters

c	Cohesion
c'	Apparent cohesion
c'_{ref}	Effective cohesion (PLAXIS 2D)
c_u	Undrained shear strength
c_{uk}	Characteristic undrained shear strength
k	Coefficient of permeability
p'_0	Effective earth pressure at rest
p_a	Active earth pressure
p_p	Passive earth pressure
p_p	Isotropic preconsolidation stress
p'	Mean effective stress
p'_f	Mean effective stress at failure
q	Deviatoric stress

q_f	Deviatoric stress at failure
u	Pore pressure
w	Weight
z	Elevation head and depth

Greek letters

ε_v	Volumetric strain
γ	Unit weight
κ^*	Modified swelling index
λ^*	Modified compression index
v	Poisson' ratio
v'	Effective Poisson's ratio
v'_{ur}	Effective Poisson's ratio for unloading/reloading
θ	Rotation angle
φ'	Angle of shearing resistance
σ	Normal stress
σ'	Effective normal stress
σ'_1	Major principle stress
σ'_3	Minor principle stress
σ'_c	Vertical preconsolidation stress
σ'_L	Limit stress
σ'_v	Vertical effective stress
σ'_{vc}	Average stress between the preconsolidation stress and the defined stress
τ_f	Shear stress at failure
ψ	Dilation angle

Abbreviations

CRS	Constant Rate of Strain
FEM	Finite Element Method
MC	Mohr-Coulomb
OCR	Overconsolidation Ratio
SLS	Serviceability Limit State
SS	Soft Soil
ULS	Ultimate Limit State

"The world which we inhabit is composed of the materials, not of the earth which was the immediate predecessor of the present, but of the earth which, in ascending from the present, we consider as the third, and which had preceded the land that was above the surface of the sea, while our present land was yet beneath the water of the ocean."

James Hutton, 1795

1 Introduction

In soft clay, excavations normally need to be supported by retaining walls. In order to minimize the need of other structural support and to reduce structural movements, the method of staged excavation is commonly used. During the construction work, it is of utmost importance that excavations are always performed in a way that guarantees safety. Except from the safety aspect, strict demands on the allowed movements in the excavation pit are commonly set.

In order to ensure that these requirements are fulfilled, complex calculations are needed. Due to the high level of complexity, hand-calculations are often complemented with numerical modelling. The finite element method is a computational procedure that includes numerical modelling. There could be great benefits when using finite element analysis software, as the design can be more efficient regarding time and costs.

1.1 Background

Several studies have indicated that fundamental knowledge of soil mechanics and numerical modelling is crucial when using the finite element method for the design of excavations (Puzrin et al., 2010; Kullingsjö, 2007; Karlsrud et al., 2005). The procedure of deriving necessary soil parameters varies depending on which constitutive model that is being used. The choice of constitutive model might in turn affect the results significantly.

Numerical modelling can be performed in both two and three dimensions, and the evaluation of excavations is in reality a three dimensional problem. This causes the calculations to be quite complex and time consuming. In order to decrease the computational time, the modelling could be done in two dimensions instead. However, two-dimensional models are sometimes based on conservative assumptions resulting in additional construction costs. It is often said that time is money, and that applies very much so to building and infrastructural projects. One way of achieving great savings, and at the same time improve the quality, is by changing working procedures in the design stage. It would therefore be beneficial to be able to simulate three-dimensional conditions of a staged excavation, only using two dimensions.

1.2 Aim and objectives

This thesis aims to evaluate the potential of using a 2.5-dimensional model in numerical modelling. The intention of the 2.5D-model is to simulate conditions and soil behaviour of a staged excavation in a reliable and efficient way, using a two-dimensional setup. This model will be calibrated against the measured deformations from an existing project. Furthermore, two different constitutive models will be compared to evaluate whether one is more beneficial than the other for the intended 2.5D-model.

1.3 Limitations

The analyses are based on the structures and conditions regarding the staged excavation at the project Tennet 2, by Skanska Sverige AB. For validation of the 2.5D-model,

measured deformations from the project are tried to be recreated, why the analyses focus on the serviceability limit states of the excavation. However, ultimate limit states are used in the back-calculation of the length of the sheet pile wall. The finite element analysis software PLAXIS 2D is used to perform the numerical modelling, in which two different constitutive models are used – the Mohr-Coulomb model and the Soft Soil model. Regarding the 2.5D-model, the cross-sections are only connected with one connection line which simulates the wailing beam.

1.4 Method

Firstly, a desk study was performed to deepen the knowledge in geotechnical engineering and the construction methodology regarding staged excavations, necessary for this work. Furthermore, the two constitutive models Mohr-Coulomb and Soft Soil were evaluated to understand their strengths and weaknesses, and to know what parameters that would be of interest when evaluating the soil tests. It was decided to use the Mohr-Coulomb model since it is common to use in order to get a first approximation of soil behaviour. According to Brinkgreve et al. (2016b), it is recommended to first use the Mohr-Coulomb model when analysing a specific problem since the computational time being relatively short. However, the Mohr-Coulomb model assumes a linear elastic perfectly-plastic stress strain relationship which may overestimate the strength of the soil, why evaluation using an additional model was needed. Since the soil at the project Tennet 2 mostly consisted of cohesive soil, it was chosen to use the Soft Soil model for further evaluation. After this, documents about the Tennet 2 project, performed by Skanska Sverige AB in Gothenburg, were analysed and evaluated. These documents constituted both description of the soil, structural elements, construction stages and measured deformations.

The finite element method software PLAXIS 2D was used to model the excavation. The modelling was based on the documents about the project. The soil parameters were partly retrieved from previous PLAXIS 2D modelling, performed by Kullingsjö (2011c) at Skanska Teknik, and partly derived from evaluating oedeometer tests. Due to insufficient data, some parameters were estimated after consultation with supervisors from Skanska Teknik and Chalmers University of Technology. To validate the model, it was compared to the earlier PLAXIS 2D model by Kullingsjö (2011c), which was used when designing the excavation for the Tennet 2 project. Furthermore, hand-calculations of the total horizontal forces on the retaining wall constituted the second validation of the model.

After this, the 2.5D-model could be simulated, which is based on a theory by A. Kullingsjö (consultation meeting, January 9, 2017) about connecting several cross-sections to evaluate three-dimensional effects. Analyses of the model were performed using both of the constitutive models. By comparing the results to the measured deformations at the construction site, it was possible to evaluate whether the 2.5D-model worked and which constitutive model giving the most accurate results. Focus was on horizontal deformations in the soil and of the retaining wall, along with generated lateral earth pressures on the retaining wall.

2 Review of soil mechanics

Soil is usually separated as either cohesive or friction soil. When there is a change of load on a cohesive soil, a momentary change of pore pressure is created which is slowly evened out by time (Knappett & Craig, 2012). This phenomenon constitutes two different states the soil may experience - drained and undrained conditions. The undrained conditions are often referred to as short-term conditions, and imply that the excess pore water pressure has not yet been evened out, which means that there is no increase in effective stress compared to before construction. Drained condition is the soil state in which excess pore water pressure has fully dissipated, and it usually refers to decades or the lifetime of the construction. In this state, the excess water has seeped out from the soil. The process where the soil reduces its volume, due to the drainage of excess water, is called consolidation. The void space in the soil is compressed, and the magnitude of the consolidation is dependent on the compression history of the soil. A soil, experiencing its greatest compression, is called normally consolidated, and a soil that has been loaded to a greater extent earlier is called overconsolidated.

In the analysis of soil stability and geotechnical design, knowledge is required about the resistance of soil to failure in shear (Commission on Slope Stability, 1995). The state of an element of soil is determined by the total normal and shear stress applied to the boundaries of the soil element (Dorf, 1996). The shear strength of a soil element is the inner resistance per unit area that the soil element can use to prevent sliding along any plane or to resist failure. For most problems regarding soil mechanics, the Mohr-Coulomb failure criteria may be used to approximate the shear strength of a soil element, see equation 2.1

$$\tau_f = c + \sigma \cdot \tan(\varphi) \tag{2.1}$$

where c is the cohesion, φ is the angle of shearing resistance, and σ is the normal stress. Equation 2.1 can be used to calculate both the drained and undrained shear strength of a soil (Sällfors, 2009). For drained conditions, the effective normal stress, σ', the cohesion intercept, c', and the friction angle, φ', are used, see equation 2.2. In undrained soil, the shearing resistance can be simplified where the undrained shear strength parameter, c_u, defines the failure envelope, see equation 2.3

$$\tau_f = c' + \sigma \cdot \tan(\varphi') \tag{2.2}$$

$$\tau_f = c_u \tag{2.3}$$

In cohesive soil, the undrained shear strength may be interpreted as a cohesion that is independent of the effective strains (Commission on Slope Stability, 1995). In normally consolidated cohesive soil, increased strains result in momentary increase of pore pressure. However, in overconsolidated soil, and at unloading of normally consolidated cohesive soil, a momentary under pressure can occur which is evened out by time. The drained strength is then, when all negative pore pressures are equalized, lower than the undrained strength, which is relevant for calculations of long time stability. This condition is usually concerned for slopes in very overconsolidated soil and for permanent excavations. Cohesive soils, like clays, have low permeability why it requires a long time for the water to drain (Duncan et al., 2014). In other words, the

shear strength in cohesive soil is dependent on time and on the overconsolidation ratio (OCR) of the soil.

2.1 Mohr-Coulomb failure criteria

For calculations where perfectly plastic behaviour is assumed, the Mohr-Coulomb failure criteria can be used (Labuz & Zang, 2012). States of stress in two dimensions can be described by a plot of effective normal stress against shear stress. Mohr's circle is defined by the effective principal stresses σ_1' and σ_3', see Figure 2.1. The line touching the Mohr circle is referred to as the failure envelope, and is described by equation 2.4. When this occurs, the soil goes from an elastic to a plastic state. As seen in the figure, c' and φ' are defining a linear relationship between effective normal stress, σ', and shear stress, τ_f.

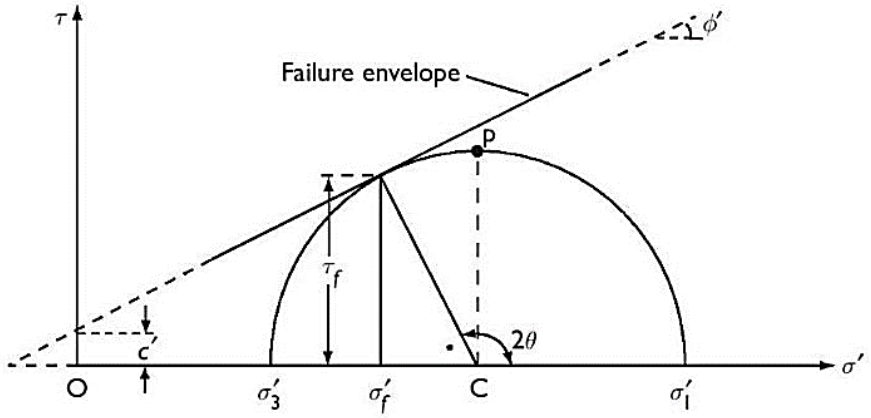

Figure 2.1 Mohr-Coulomb failure criterion in stress-strain relationship (Knappett & Craig, 2012).

Shearing resistance in the soil is developed by interparticle forces (Knappett & Craig, 2012). This causes for the shearing resistance to be equal to zero kPa if the effective normal stress and the cohesion are zero kPa. This point is crucial to the interpretation of shear strength parameters. From the geometry of the Mohr circle, the Mohr-Coulomb failure criteria can be expressed in terms of the relationship between the principal stresses:

$$\sigma_1' = \sigma_3' \cdot tan^2\left(45° + \frac{\phi'}{2}\right) + 2c' \cdot tan\left(45° + \frac{\phi'}{2}\right) \quad (2.4)$$

When a load is rapidly applied on a clay, relative the time for drainage, the conditions are undrained. The shear strength, τ_f, in an undrained soil can be expressed in terms of total stresses (Sällfors, 2009). The value of c_u depends on the previous history of the soil layer, the way the load is changed, and the geostatic stress state (Smoltczyk, 2002). This leads to the failure envelope being horizontal instead of having an inclination, see Figure 2.2, and the soil starts yielding when the undrained shear strength, c_u, is exceeded.

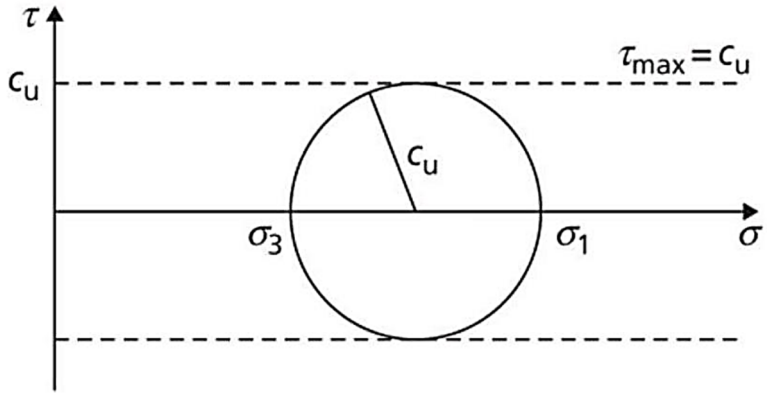

Figure 2.2 Mohr circle, failure criteria for undrained case (Knappett & Craig, 2012).

2.2 Lateral earth pressure

In the analyses of retaining walls, the change in earth pressure due to movement is taken into account by splitting up the surrounding soil into two different sides - the active and the passive side, see Figure 2.3 (Knappett & Craig, 2012). The lateral earth pressures are dependent on the potential movements of the wall, and are calculated with the use of earth pressure coefficients. The lateral earth pressures on the active side cause for the retaining wall to move, and the pressure on the passive side counter these movements. When the wall moves, the pressure on the active side reduce, while it increases on the passive side.

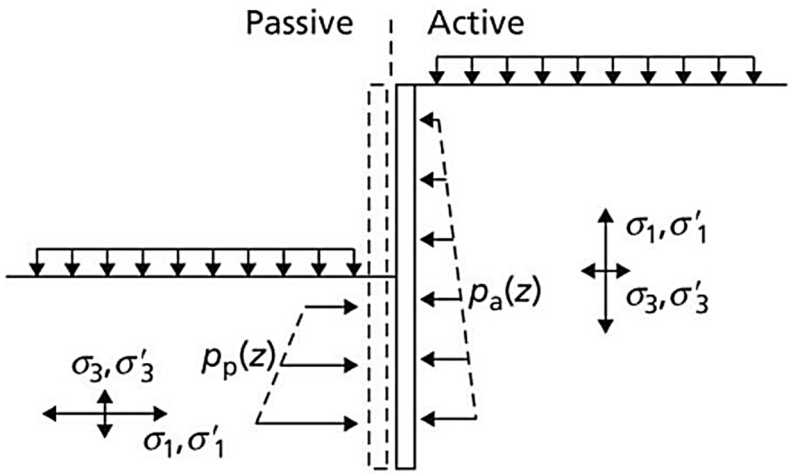

Figure 2.3 Active and passive earth pressures (Knappett & Craig, 2012).

Note that on the passive side σ_3' represents the vertical stress and σ_1' represents the horizontal stress, while on the active side it is vice versa. The lateral earth pressures can be calculated based on Terzaghi's principle (1925) and the theory of Rankine (1857). When the horizontal respectively the vertical stress become equal to the active respectively the passive pressure, the soil is called to be in a Rankine state. Due to the friction angle of the soil, an active and passive earth pressure coefficient are used to calculate the lateral earth pressures, see equation 2.5 and 2.6

$$K_a = \frac{1-sin\phi}{1+sin\phi} \tag{2.5}$$

$$K_p = \frac{1+sin\phi}{1-sin\phi} \tag{2.6}$$

However, Rankine's theory is based on a set of assumptions and simplifications. It is assumed that there is no friction on the wall and that the ground and failure surfaces are straight planes (Bartlett, 2010). It is also assumed that there is no friction acting between the soil and the backfill. This leads to the Rankine's theory not being completely accurate for calculation of earth pressures directly against a wall. It is instead better for calculation of earth pressures on a vertical plane within a mass of soil. When it is desired to calculate the resultant horizontal force acting on a retaining wall, it could be more feasible to use the Coulomb theory (1776). This theory takes the slope of the wall, interface friction angle between the soil and the wall, and slope of backfill into account. The assumption that soil shear resistance develops along the wall and failure plane is the basis of this theory. However, according to A. Kullingsjö (consultation meeting, March 6, 2017), when calculating the lateral earth pressures with Terzaghi's principle using Rankine's theory, the plausible friction can be integrated by adding the interface parameter, R, as can be seen in equation 2.7 and 2.8

$$p_a = K_a(\int \gamma dz - u) - 2\sqrt{K_a}c'\sqrt{1+\frac{2}{3}R} + u \tag{2.7}$$

$$p_p = K_p(\int \gamma dz - u) + 2\sqrt{K_p}c'\sqrt{1+\frac{2}{3}R} + u \tag{2.8}$$

R may range from zero to one, and describes the interface between an undrained cohesive soil and the construction. Note that equation 2.7 and 2.8 are general equations for calculation of the lateral earth pressure, and should be varied according to present drainage condition. As mentioned before, for undrained conditions, the friction angle is equal to zero degrees, which results in K_a and K_p being equal to one according to Rankine's theory. Moreover, no coefficient is used to recalculate the earth pressure, caused by the groundwater, from vertical to horizontal. This is because the magnitude of the groundwater pressure is the same in all directions.

If the strains in the lateral direction are zero, the lateral earth pressure is called to be at-rest (Knappett & Craig, 2012). At this state, a new variable is introduced called the coefficient of earth pressure at-rest, K_0. For normally consolidated clays, this coefficient was proposed by Jaky (1944) to be calculated according to equation 2.9

$$K_{0,nc} = 1 - \sin\phi' \tag{2.9}$$

However, due to the stress history, the soil might be overconsolidated and the coefficient K_0 is then greater than unity (Knappett & Craig, 2012). In Eurocode 7, Orr and Farrell (2012) proposed to calculate K_0 according to equation 2.10

$$K_0 = (1 - \sin\phi')\sqrt{OCR} \tag{2.10}$$

For both normally and overconsolidated clays, the effective earth pressure at-rest, p_0', is calculated according to equation 2.11

$$p_0' = K_0 \sigma_v' \tag{2.11}$$

As mentioned above, the active pressure is a result of lateral expansion of the soil at failure, while passive pressure correlates to lateral compression of the soil at failure (Knappett & Craig, 2012). These pressures are referred to as limit pressures; the active lateral earth pressure is a minimum value, and the passive lateral earth pressure is a maximum value. Figure 2.4 illustrates the relationship between lateral strain and the three lateral pressure coefficients.

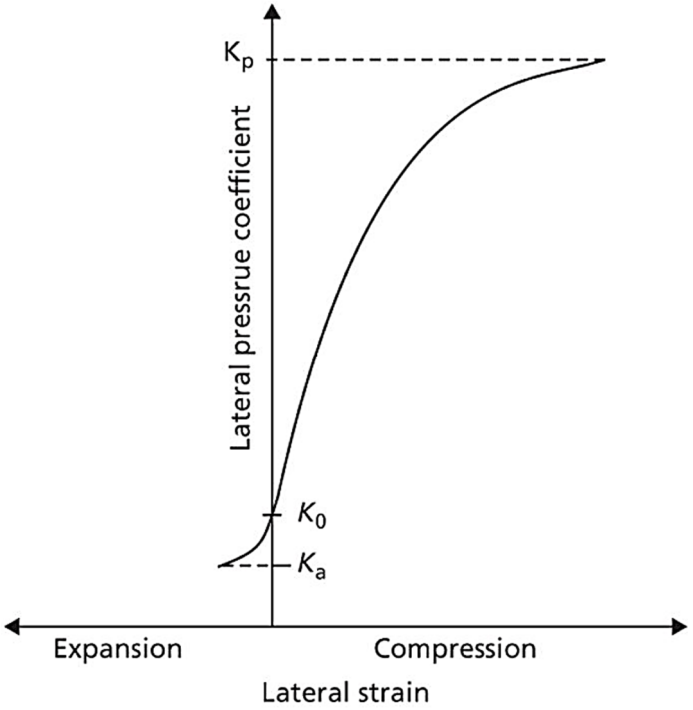

Figure 2.4 Relationship between lateral strain and lateral pressure coefficient (Knappett & Craig, 2012).

3 Review of construction methodology

In this section, the components involved in a retaining structure are presented, along with the concept staged excavation. The components are the same as in the evaluated Tennet 2 project, and can be viewed in Figure 3.1. Furthermore, the finite element program PLAXIS 2D together with the Mohr-Coulomb model and the Soft Soil model are also described.

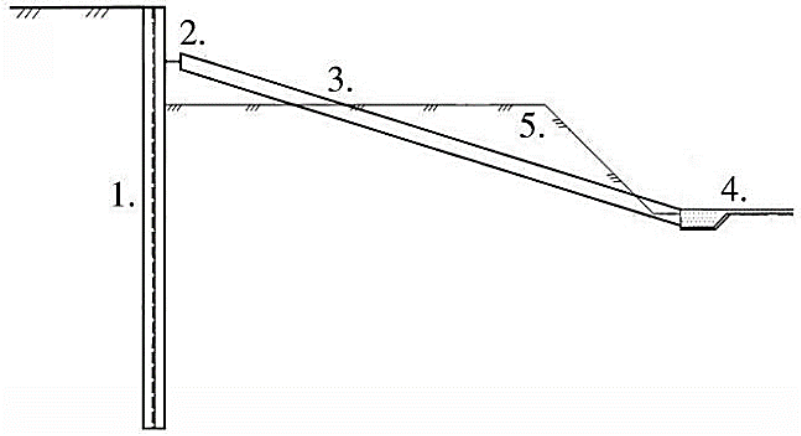

Figure 3.1 The different components of the excavation in the Tennet 2 project. 1) Sheet pile wall 2) Wailing beam 3) Prop 4) Casted concrete 5) Berm.

3.1 Retaining structure

The purpose of an earth-retaining structure is to prevent, according to the principles of limit state design, all types of collapse or major damage of the structure. It should also prevent deformations unacceptable for the function of the structure, and at the same time endure damage that would require excessive maintenance.

The design of a retaining structure can be determined by two different criteria; ultimate limit state (ULS) and serviceability limit state (SLS) (Orr & Farrell, 2012). Both criteria must be considered. The design of earth retaining structures must fulfil practical aspects of the construction and prevent excessive deformations. This is taken into consideration when evaluating SLS. Furthermore, ULS concerns the design against brittle failure, in other words sudden collapse of one component or the whole structure. There can be two different failure types considering the ULS; failure of the structural elements or failure in the soil, which is the most common. These limit state criteria constitute for the basis when designing a retaining wall.

There are two extensive types of retaining structures, whereof one is gravity wall in which the stability is mainly relying on the self-weight of the structure (Knappett & Craig, 2012). The second type is embedded wall in which stability relies on the passive resistance of the soil over the embedded depth, and in some cases on external support. The embedded wall type is the one that was used for the Tennet 2 project.

Factors of safety, in terms of the ratio between restoring and overturning moments, are used in the design of retaining structures. These factors are traditionally very conservative due to the uncertainties regarding soil properties, and include actions in

loading, in-situ stresses, self-weight of the soil, pore water pressure, seepage pressure and ground movements. These uncertainties can be compensated for by the usage of partial coefficients, which are used to recalculate the properties of the soil in a conservative point of view. The approach is in most cases to base the design of the structure on the ultimate limit states, in that way the serviceability limit state requirements are generally satisfied.

Retaining wall

When calculating the stability of the retaining wall and the included structural parts, it is necessary to calculate the resulting earth pressure for both the active and passive side (Ryner et al., 1996). Calculations of the lateral earth pressures can be done using Rankine earth pressure as basic earth pressure, which is then corrected for every arisen loading situation. The earth pressure, in combination with a possible water pressure, constitute the forces that acts on the retaining wall. In order to fulfil horizontal and moment equilibrium for a sheet pile wall without anchoring, it is necessary to implement the retaining wall at such a depth that the earth pressures on the active side respectively on the passive side balance each other.

Wailing beam

The purpose of a wailing beam is to distribute the horizontal load along the sheet pile wall (Ryner et al., 1996). When designing a wailing beam, the loading is calculated by evaluating the earth and water pressures. When calculating the total loading of the wailing beam, consideration should be taken to the deformation dependence of the earth pressure. This deformation dependence is handled differently in ultimate limit states respectively serviceability limit states, and for every evaluated fracture model.

Prop

Props are used as support for the sheet pile wall during the excavation. They are usually connected between the wailing beam and fixed structures in the centre of the excavation. After the construction, the props can either be removed or left for further support. The props are dimensioned on basis of the loading of the wailing beam (Ryner et al., 1996).

3.2 Staged excavation

Staged excavation is a method where the stability of the soil is utilised combined with external support. There are several different ways to perform staged excavation, and the principle presented in this thesis involves one segment at a time being excavated and replaced by a concrete slab combined with props. This process is then continued along the wall in the most feasible way regarding safety and costs.

Berm

The usage of berms is a technique to establish passive pressure against retaining walls. This decreases the risk of the excavation collapsing. The berm is sequentially removed along with the casting of coarse concrete, why it is called staged excavation. The dimensions of this pressure bank vary in relationship to the structure and depth of the excavation.

Casting of coarse concrete

Embedded walls are dependent on movements to function (Commission on Slope Stability , 1995). The retaining wall rotates around a point above the lower edge, why the required movement is highly dependent on the chosen embedded depth. To decrease the movement, coarse concrete can be casted against the retaining wall. It is recommended to first cast a part of the prospected baseplate and to leave a slope against the wall (Ryner et al., 1996). After this, the excavation is done in different stages so that more of the retaining wall is exposed, sequentially with coarse concrete being casted between the retaining wall and the baseplate. After the final excavation stage, coarse concrete has been casted against the retaining wall all along the stretch.

Strains in the retaining wall and concrete are calculated with the simplifying assumption that the level of the coarse concrete can be seen as a symmetry line for the forces (Commission on Slope Stability , 1995). The movements that are being produced before the casting have had a point of rotation at greater depths, but after the casting, the rotation will be around the coarse concrete. This results in a change in the forces acting under the excavation bottom, which conservatively can be applied as a mirrored earth pressure as long as the embedded depth is equal to or greater than the excavation depth.

3.3 Numerical modelling with PLAXIS 2D

When dealing with complex geotechnical problems, numerical methods of mathematics can be a feasible option to evaluate different construction scenarios. This is because numerical modelling is in general more suitable for complex problems than classical analytical methods (Smoltczyk, 2002).

The finite element method (FEM) is a computational procedure, including numerical modelling, that enables for an approximate solution to a specific boundary value problem (Karstunen, 2016). The approximation is based on algebraic equations that involve many different variables, concerning geotechnical engineering. These variables can for example be soil and structural parameters, and they are evaluated at several discrete points called nodes within the region of interest. Depending on the desired level of complexity, the number of nodes being evaluated can be monitored. The finite element equations are constructed to minimise the error in the approximate solution.

PLAXIS 2D is a finite element method software, that is used to carry out two-dimensional finite element analyses of geotechnical problems. A plain strain model is used when studying geometries with a uniform cross section, meaning that the corresponding stress state and loading scheme are uniform for a certain length, perpendicular to the z-direction (Brinkgreve et al., 2016b). A limitation when using the two-dimensional plain strain model is that the displacements and strains in the third dimensions are assumed to be zero, but the normal stresses are not. Moreover, the soil is divided into many different elements, each with its own set of nodes. Each node has specific degrees of freedom (Karstunen, 2016). The soil originally consists of an infinite number of elements, with an infinite number of degrees of freedom. The FEM decreases the number of elements, resulting in the soil having a finite number of degrees of freedom. In other words, FEM enables for discretisation of something that is continuous. This method enables for calculation of displacements and strains at the nodes, and stresses at so-called Gauss points.

When both the soil and structural input is set in PLAXIS 2D, the geometry has to be divided into finite elements. The composition of these finite elements is called a mesh, and the level of coarseness may be varied (Brinkgreve et al., 2016b). It is important that the mesh is fine enough to generate accurate results, and it should be finer around more complex structural areas. However, the computational time increases with an increase in finite elements.

Furthermore, it is possible for the user to define what different construction phases there are. This can for example be an activation of a specific loading type at a certain time, or the simulation of a retaining wall being implemented in the soil during a period of time etc. For each phase, the user may set the desired type of analysis. Also, it is possible for the user to define specific boundary conditions for a selected phase. These boundary conditions involve for example deformations and groundwater flow.

3.3.1 The Mohr-Coulomb model

When using the Mohr-Coulomb model in PLAXIS 2D, five parameters are required as input (Brinkgreve et al., 2016b). These five parameters can be retrieved by analysing basic soil tests, and they constitute of two stiffness parameters and three strength parameters. The effective stiffness parameters are

E'	Effective Young's modulus	[kN/m^2]
v'	Effective Poisson's ratio	[-]

The effective strength parameters that are necessary for the Mohr-Coulomb model are

c'_{ref}	Effective cohesion	[kN/m^2]
φ'	Effective friction angle	[^{o}]
ψ	Dilation angle	[^{o}]

In PLAXIS 2D, it is possible to model undrained behaviour based on effective stiffness and strength parameters using the drainage type Undrained (A) (Brinkgreve et al., 2016b). The undrained shear strength, c_u, is for this drainage type based on the drained strength parameters, and automatically estimated. Since the Mohr-Coulomb model assumes isotropic elastic behaviour during pre-failure deformation, the generated pore water pressures may be unrealistically low (Puzrin et al., 2010). This causes for the effective stresses to be constant, and the stress path to failure becomes vertical in the triaxial stress space, see Figure 3.2. However, in reality, normal- to slightly overconsolidated clays are not isotropic, and they have a tendency to contract during drained loading. This would in undrained conditions cause for positive excess pore water pressures since water is incompressible. As can be seen in Figure 3.2, when comparing q_f between (a) and (b), this causes for the undrained strength to be overestimated when modelling with the Mohr-Coulomb model. Due to this consequence of the model and lack of knowledge in numerical modelling, this was the cause for the collapse of Nicoll Highway in Singapore 2004 (Puzrin et al., 2010).

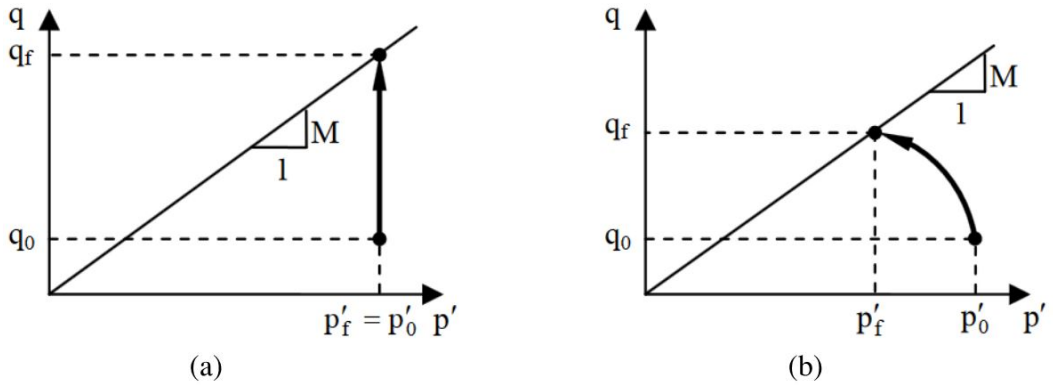

Figure 3.2 Undrained effective stress path: (a) Mohr-Coulomb model; (b) normally consolidated clay (Puzrin et al., 2010).

It is also possible to model undrained behaviour based on effective stiffness and undrained strength parameters. This is done by using the drainage type Undrained (B). Note that the undrained strength parameters are not presented above. The undrained shear strength, c_u, is for drainage type Undrained (B) manually typed in, and the friction and dilation angles are automatically set to zero degrees. This enables for the undrained shear strength to be estimated more similar to (b) in Figure 3.2. When using this drainage type, the prediction of pore pressures may be highly inaccurate, which makes this option inappropriate for consolidation analysis.

3.3.2 The Soft Soil model

When constructing on soft soils, like normally consolidated clays, clayey silts, or peat, regard must be taken to the high compressibility of the soil (Brinkgreve et al., 2016a). In PLAXIS 2D, the Soft Soil model is such a model that is useful if the time aspect is of minor importance. The model accounts for elastic and plastic strains and is useful in consolidation analysis, but less suitable when accounting for creep. The model is based on the Modified Cam Clay model, using the Mohr-Coulomb failure criteria. The Modified Cam Clay model is based on drained triaxial tests and is presented in the invariants p' and q, which are the mean effective and deviatoric stress, where the deviatoric stress describes the distortion of the soil body.

In the Soft Soil model, a logarithmic relationship between the mean effective stress and volumetric strain is assumed (Neher & Wehnert, 2001). The relationship can be determined by the modified compression index parameter, λ^*, and the modified swelling index parameter, κ^*, which are the stiffness parameters for the Soft Soil model

λ^*	Modified compression index	[-]
κ^*	Modified swelling index	[-]

λ^* and κ^* can be determined from the oedoemeter tests showing unloading/reloading, where λ^* is related to the virgin compression line and κ^* is related to the unloading of the soil, see Figure 3.3. These parameters are inverted related to the stiffness, meaning that the lower the value of λ^* and κ^* the greater the stiffness (Brinkgreve et al., 2016a). The modified swelling index is together with Poisson's ratio used as input in the Soft Soil model to compute the elastic strains. The preconsolidation stress, p_p, is the largest stress the soil has experienced and remains constant during the unloading/reloading. At

primary loading however, p_p increases with the additional stress causing plastic volumetric strains.

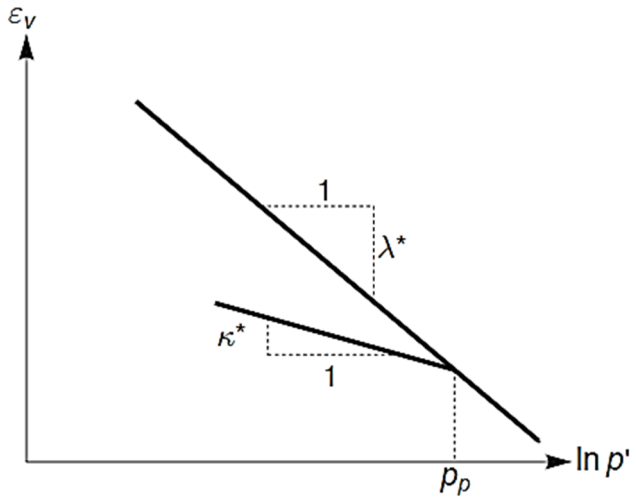

Figure 3.3 Logarithmic relation between volumetric strain and mean stress (Brinkgreve et al., 2016a).

To model the failure state in the Soft Soil model, a perfectly-plastic Mohr-Coulomb yield function is used (Neher & Wehnert, 2001). The top of the yield surface is located on a line with inclination M, see Figure 3.4. This is the critical state line that represents the stress states at post peak failure. In Figure 3.4, the yield surfaces of the Soft Soil model are shown, where the bold lines represent the elastic boundaries. The Mohr-Coulomb failure line is fixed, but the cap may increase in primary compression.

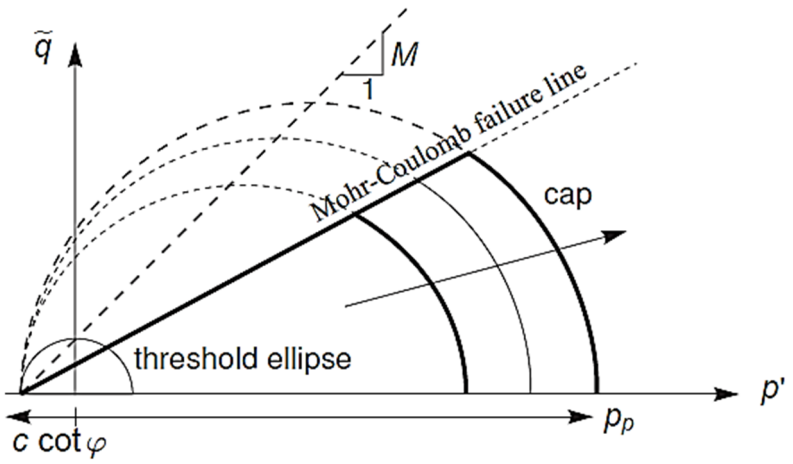

Figure 3.4 Yield surfaces of the Soft Soil model in p'-q-plane (Brinkgreve et al., 2016a).

The failure criteria for the Soft Soil model is however not necessarily related to the critical state. It is instead the same as for Mohr-Coulomb, described by the strength parameters

c'_{ref}	Effective cohesion	[kN/m^2]
φ'	Effective friction angle	[^{o}]
ψ	Dilatancy angle	[^{o}]

4 Modelling of the staged excavation

In this thesis, the behaviour of the staged excavation related to the project Tennet 2 was analysed using the finite element software PLAXIS 2D. Two different constitutive models were used in PLAXIS 2D – the Mohr-Coulomb and Soft Soil model. In order to validate that the ground conditions were modelled correctly in PLAXIS 2D, hand-calculations were performed. In this section, the input data for both the constitutive models is presented. Furthermore, the modelling of the excavation and the corresponding construction phases are explained.

4.1 Tennet 2

In 2011, Skanska Sverige AB did a project called Tennet 2 in Gothenburg (Hansson, 2011b). This project included staged excavation, and was the basis for the simulations performed in this report. Tennet 2 constitutes an office building, consisting of six floors with an additional basement. Blueprints of the construction site can be found in Appendix A. The chosen section to evaluate was section A-A, see Figure A.1 in Appendix A.

Site description

The property of Tennet 2 has a total area of about 2500 m^2 and was since 1985 used as a parking area (Hansson, 2011b). Tennet 2 is adjacent directly to the office building called Tennet 1 in the west, and in the east to the street Kämpegatan. In the north and south, the property is adjacent to asphalt paved areas, which in turn boarders on buildings with offices and trading activities. The location of Tennet 2 can be seen in Figure 4.1.

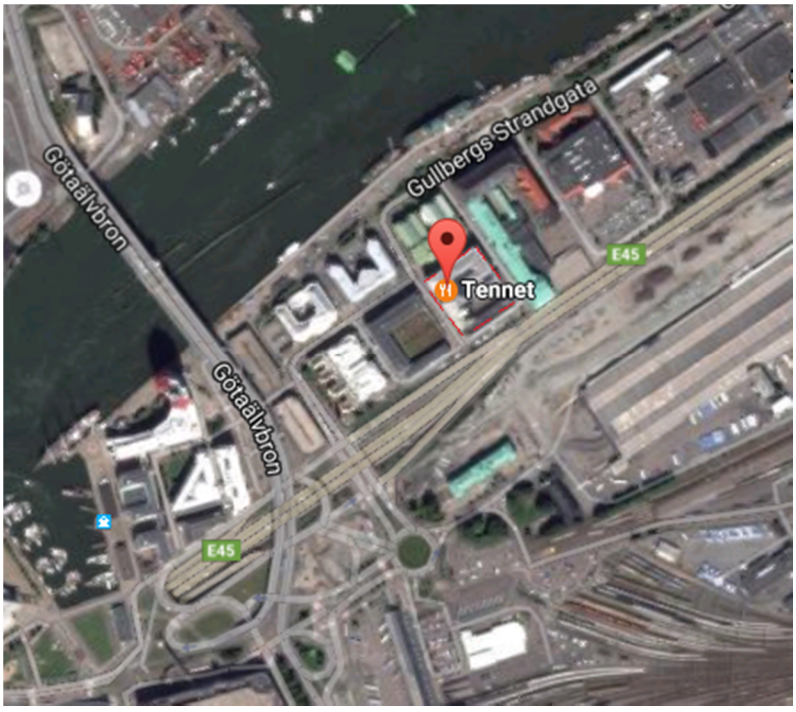

Figure 4.1 Location of the Tennet 2 building (GOOGLE MAPS, 2017).

The area is since the mid-1800s a padded reeds area adjacent to the Göta River (Hansson, 2011b). Due to this, the groundwater level in the superficial layers of filling is largely dependent on the water level in the Göta River. The average water level in the river is located at +10.1 meter. The area has previously been colonised and different kinds of activities have been conducted here. The land is generally flat with surface levels between +11.2 and +11.9 meters. The soil layers comprise of fill material at the top, which thickness in the surveyed points varies between 1.6 and 2.7 meters. In the superficial layers, sand and gravel with elements of brick and concrete dominate. Contents of clay and mud increases with depth, and basic residues from previous buildings exist in the soil. The natural soil layers are composed of clay into great depth. Soundings have been driven down to just over 55 meters without stop. Down to about 5 meters, the clay is muddy and has elements of shells.

The undrained shear strength of the clay ranges from 17 to 60 kPa (Hansson, 2011b). Thus, the strength of the clay is very low in the upper layers, increasing to medium-high at 40 meter depth. The sensitivity of the clay ranges between 8 and 18, hence the clay is relatively sensitive. The natural water content of the clay is highest closest to the filling where it amounts to about 80%, and then decreasing to about 60-70%.

Performed Constant Rate of Strain (CRS) tests show that, for the measured pore pressure, some consolidation settling is present at around 15 meter depth, while the clay at greater depths is slightly overconsolidated (Hansson, 2011a). In addition to remaining consolidation settlements, secondary settlements is on-going due to the laid filling. The compression modulus, M_L, varies between 650 and 900 kPa.

Construction description

In order to obtain satisfying safety and stability, a 12 meter long sheet pile wall was stabilised with a prop connected to the coarse concrete that was casted in the middle of the excavation (Edmark & Hansson, 2011a). The desired length of the sheet pile wall had been calculated by using a specific set of partial factors for the soil and structure properties. In addition, a surface load of 10 kPa, placed in favour of failure, had been taken into account when dimensioning the sheet pile wall. This length resulted in a safety factor of 1.45, see Figure A.2 in Appendix A. In order to ensure a satisfying stability, staged excavation was performed. This included the implementation of berms against the sheet pile wall, which were then sequentially excavated and replaced with coarse concrete. The thickness of the concrete slab was 0.1 meter.

The excavation and the installation procedure of the sheet pile wall, with all components, were described in the construction document by Edmark et al. (2011b). In order to be able to simulate only a few of the excavation cuts, the procedure has been simplified in this thesis

1. Installation of the sheet pile wall
2. Excavation to the top level of the berms
3. Piling in the centre of the excavation
4. Excavation in the centre to the final depth
5. Casting of the coarse concrete in the centre of the excavation
6. Installation of the wailing beam
7. Anchoring of the props against the coarse concrete
8. Sequential removal of the berms, and casting of the coarse concrete against the sheet pile wall
9. Removal of the props.

The procedure is shown in Figure 4.2.

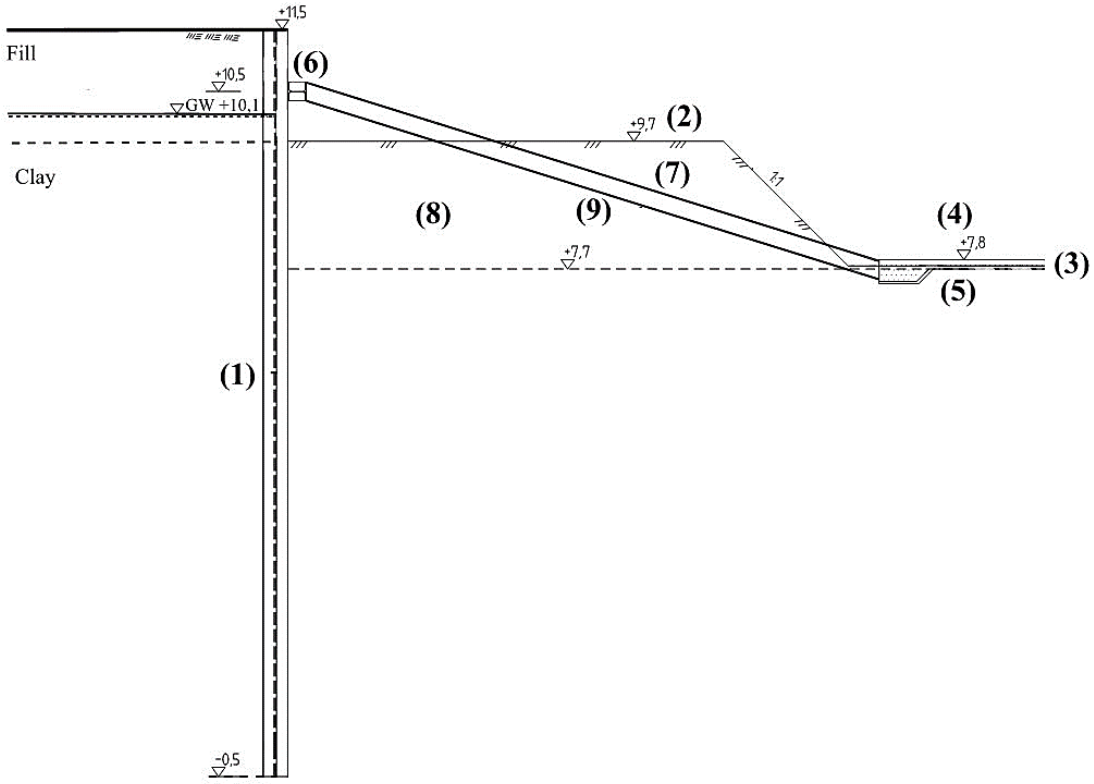

Figure 4.2 Cross-section and procedure of the excavation (Edmark et al., 2011b [modified]).

Based on the calculations performed by Edmark and Hansson (2011a), the sheet pile wall was chosen to be of type PU12-R, S355GP, the props and wale of type HEB300, S355JO, and the quality of the concrete was C25/30.

For this thesis, the total time frame for the project and the time for each construction stage were approximated after consultation with M. Johansson (personal communication, March 14, 2017) and by old notes from the project. The excavation procedure stretched from approximately 2011-09-13 to 2011-12-03. Before the excavation to the final depth in the centre, piles were installed in the ground. During the time in which the piles were installed, the rest of the work with the excavation was at hold.

Measured deformations

In Appendix A, blueprints of the construction site can be found. For the analyses, performed in this report, cross-section A-A was evaluated, see Figure A.1 in Appendix A. At this section, three nodes were placed on the wailing beam during the project, which were used to measure the movements before and during the excavation. Soon after the excavation was finished, piles were put down inside of the excavation. This lead to an earth pressure pushing the wall away from the excavation, resulting in a misleading deformation of the sheet pile wall. Therefore in this thesis, the graphs were modified during the dates for when the piles were put down in the excavation, hence the horizontal parts in the beginning of the deformations in the diagram. The spikey parts in the graphs were most likely caused by disturbances at the construction site.

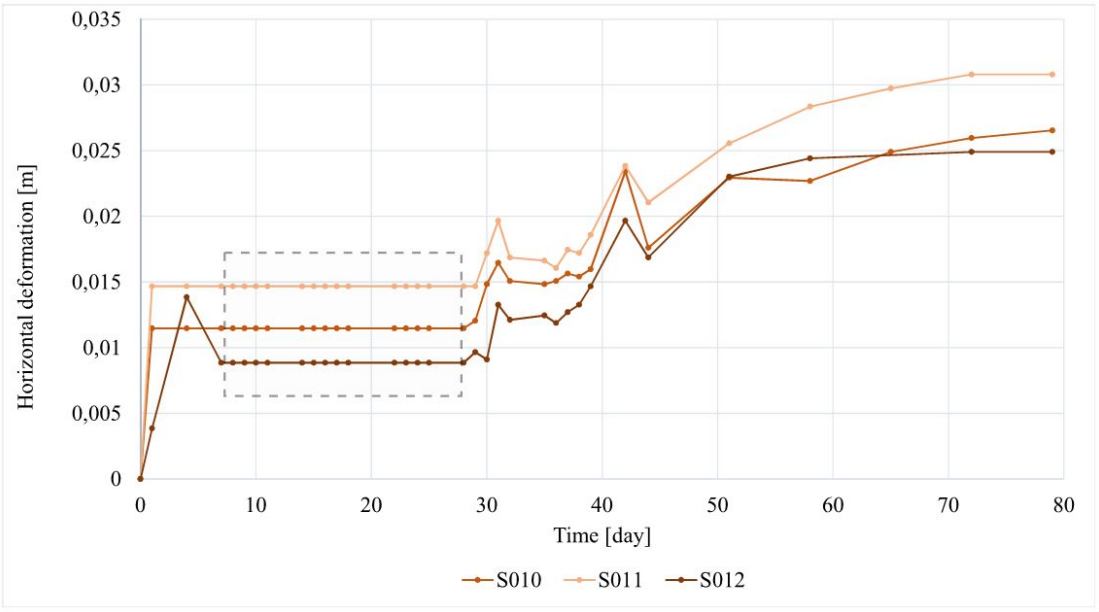

Figure 4.3 *The measured deformations of the sheet pile wall, at the level of the wailing beam (Kullingsjö, 2011b [modified]). The box represents the time when the piling was performed.*

Furthermore, during the construction, an inclinometer K4 was installed close behind the sheet pile wall that registered horizontal deformation in the soil by depth over time. The first measuring was made at the day the sheet pile wall had been completely installed. The measured values of these deformations can be seen in Figure 4.4.

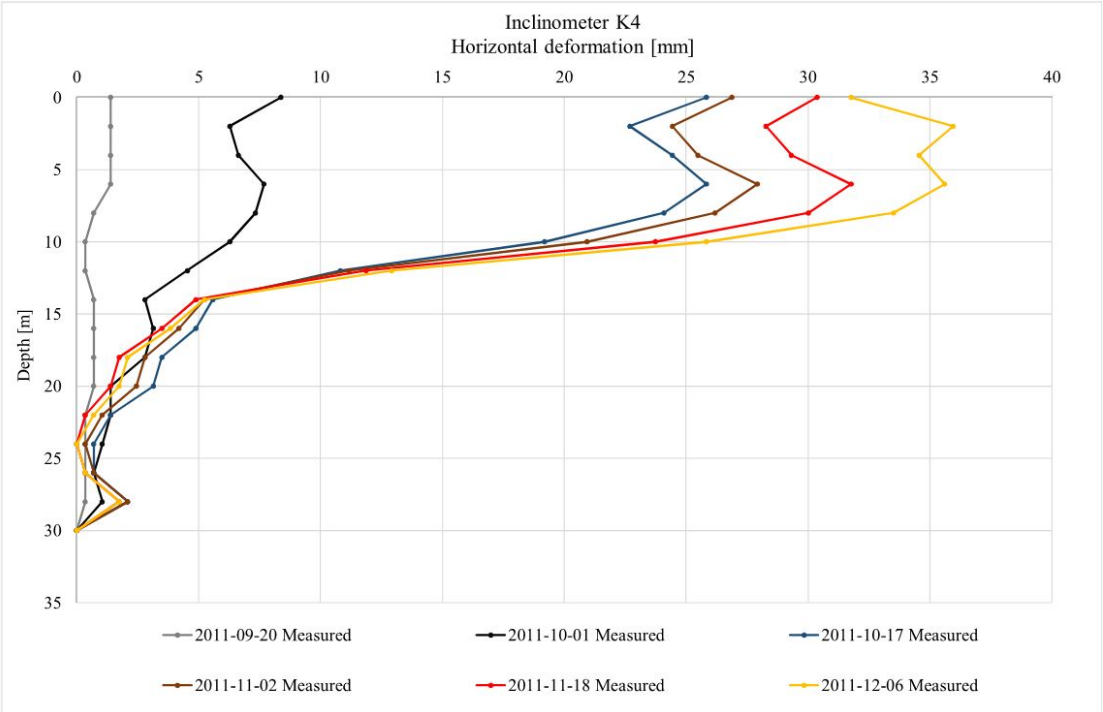

Figure 4.4 *Measured deformations by depth, behind the sheet pile wall (Kullingsjö, 2011a [modified]). These deformations were also modified regarding the piling.*

4.2 Input data Mohr-Coulomb model

The necessary data for deriving soil parameters was found in the project description documents by Hansson (2011b). However, the drained soil parameters were not given in the documents, which resulted in them being assumed after consultation meetings with Skanska Teknik.

Five different soil layers can describe the stratigraphy at the construction site; one containing fill material and four clay layers with different characteristic values (Hansson, 2011b). By calculating an increase per metre between the layers, linear interpolation was made regarding c_u, c' and E'. According to the previous modelling of Tennet 2 in PLAXIS 2D by Kullingsjö (2011c), the value of E' was based on the unloading modulus, E_{ur}, and empirically estimated according to equation 4.1

$$E_{ur} = 500 c_u \tag{4.1}$$

This is however a quite rough estimation that was done for all layers, and it should be noted that the stiffness in fact varies with strain. There is no analytical correlation between the stiffness and the undrained shear strength, but an empirical estimation that is commonly used for clays in Gothenburg. According to Ismail and Teshome (2011), it is also possible to use an empirical approach based on the preconsolidation stress, σ_c', equation 4.2, for estimation of the stiffness modulus

$$E_{ur} = (2\ to\ 3) \cdot 50 \sigma_c' \tag{4.2}$$

The data in Table 4.1 was used as input when modelling the excavation in PLAXIS 2D using the Mohr-Coulomb model Undrained (B).

Table 4.1 Input data for the Mohr-Coulomb model Undrained (B) (Kullingsjö, 2011c).

	Unit	Fill	Clay 1	Clay 2	Clay 3	Clay 4
Level		+11.5 / +9.7	+9.7 / +6.0	+6.0 / +0.0	+0.0 / -13.0	-13.0 / -20.0
Material behaviour	-	Drained	Undrained (B)	Undrained (B)	Undrained (B)	Undrained (B)
γ	[kN/m^3]	18 / 21	15.5	16	16.5	16.5
c_u	[kN/m^2]	-	17	17	21	37
E'	[kN/m^2]	1×10^4	8500	8500	1.05×10^4	1.85×10^4
ν'	[-]	0.3	0.2	0.2	0.2	0.2
c'_{ref}	[kN/m^2]	1.0	-	-	-	-
φ'	[°]	30	-	-	-	-
ψ	[°]	0	-	-	-	-

When using the drainage type Undrained (A), the friction angle was assumed to be 30 degrees for all soil layers, see Table 4.2. This assumption might have caused for the strength of the soil to be slightly overestimated. However, according to T. Edstam (consultation meeting, March 20, 2017), a friction angle close to 30 degrees is quite common for clays why it can be seen as a standard assumption. The cohesion, c', was assumed to be a tenth of the undrained shear strength, c_u, for all layers. The same input data as for Undrained (A) was used for the drained analyses.

Table 4.2 Input data for the Mohr-Coulomb model Undrained (A) and Drained (Kullingsjö, 2011c).

	Unit	Fill	Clay 1	Clay 2	Clay 3	Clay 4
Level		+11.5 / +9.7	+9.7 / +6.0	+6.0 / +0.0	+0.0 / -13.0	-13.0 / -20.0
Material behaviour	-	Drained	Undrained (A) / Drained	Undrained (A) / Drained	Undrained (A) / Drained	Undrained (A) / Drained
γ	[kN/m^3]	18 / 21	15.5	16	16.5	16.5
E'	[kN/m^2]	1×10^4	8500	8500	1.05×10^4	1.85×10^4
ν'	[-]	0.3	0.2	0.2	0.2	0.2
c'_{ref}	[kN/m^2]	1.0	1.7	1.7	2.1	3.7
φ'	[°]	30	30	30	30	30
ψ	[°]	0	0	0	0	0

4.3 Setup of initial model

After the different parameters for the Mohr-Coulomb model had been determined, it was possible to set up an initial model in PLAXIS 2D. For this model, drainage type (B) was chosen, and the aim was to ensure that the basic conditions were modelled correctly in PLAXIS 2D. To validate this, the generated earth pressures, acting on the sheet pile wall, were compared to hand-calculations.

Simulation of earth pressure in PLAXIS 2D

The model in PLAXIS 2D was simplified by excluding the wailing beam, props and concrete. Moreover all of the soil was simulated to be excavated at one time. The resulting forces on the wall calculated in PLAXIS 2D can be seen in Figure 4.5.

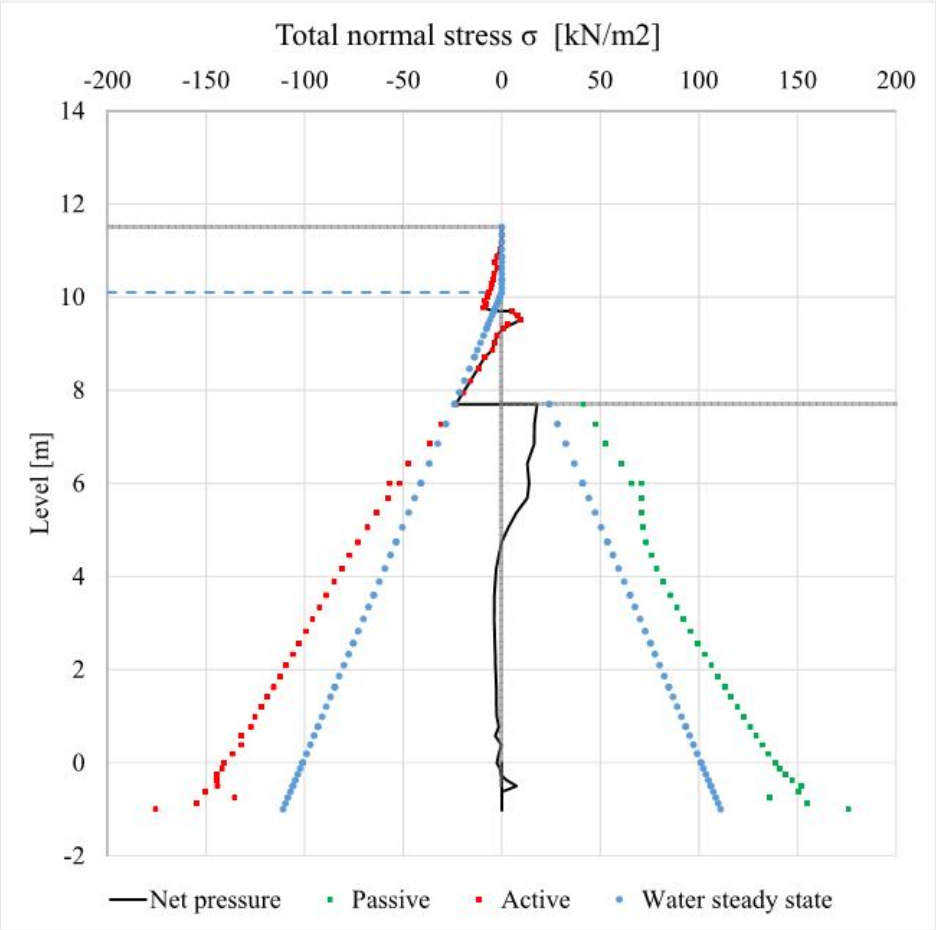

Figure 4.5 Lateral earth pressures, calculated with initial model.

It can be seen in Figure 4.5 that the active earth pressure at the level of the groundwater table was negative. This earth pressure generation caused for the retaining wall to be subjected to suction at the top. As seen from equation 2.7, the cohesion is subtracted when calculating the active earth pressure. This results in a negative active pressure close to the surface, where the cohesion is greater than the stress. However, this was not desired and a flaw simulated in PLAXIS 2D. According to A. Kullingsjö (consultation meeting, April 5, 2017), the drawback could be solved by setting the drainage type of the interfaces between the soil and sheet pile wall to be drained. By doing this, the tension cracks in the soil were taken into account. In order to not overestimate the stability of the retaining wall, tension cracks should always be taken into consideration during the design (Commission on Slope Stability, 1995; Orr & Farrell, 2012). The updated setting for the interface resulted in effective parameters for soil being used when calculating the earth pressures.

To define the interaction between two materials, in PLAXIS 2D, the interface value, R_{inter}, can be set. This parameter is related to R, found in equations 2.7 and 2.8. After looking at suggested reduction factors by Brinkgreve and Shen (2011), the input parameters were set to 0.5 for the drained interfaces as they simulated the friction between the steel and the clay. The interfaces for the rest of the soil layers were set to 1.0. The resulting earth pressures, after updating the model, are shown in Figure 4.6.

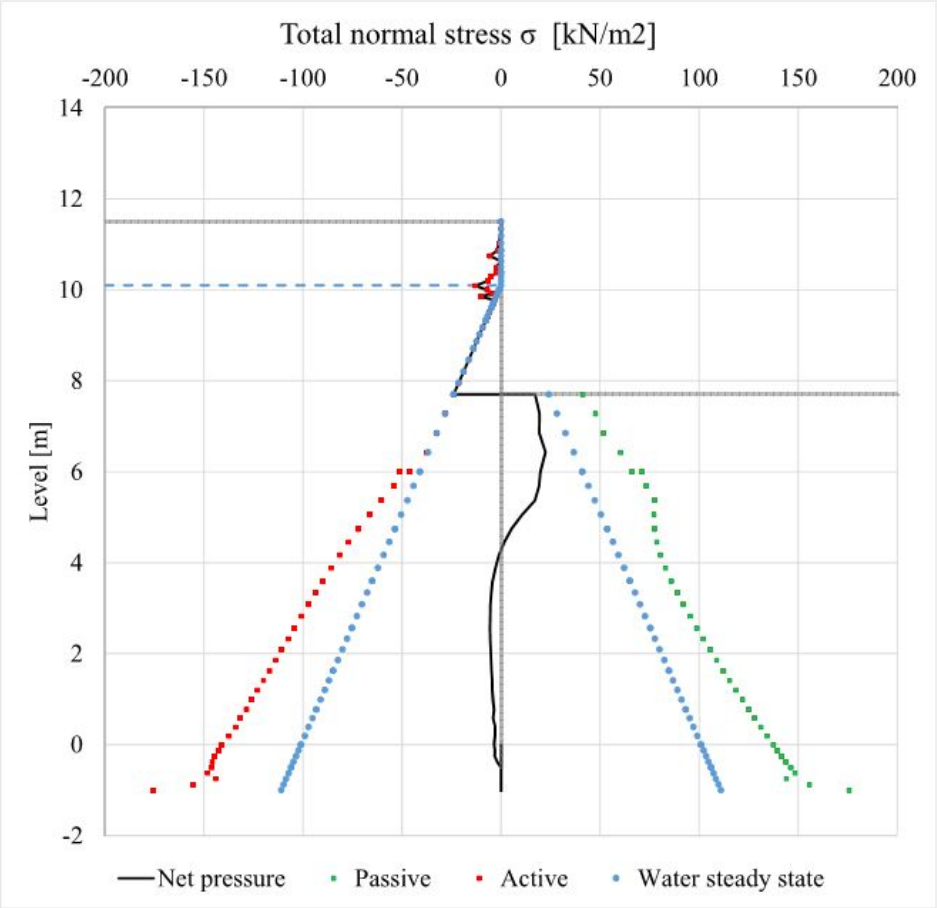

Figure 4.6 Lateral earth pressures, calculated with updated model.

Simulation of earth pressure by hand-calculations

In order to verify that the pressures generated in PLAXIS 2D were reasonable, these were also calculated by hand, using the equations 2.5 to 2.8. The hand-calculations in this thesis are based on Rankine's theory, as they are only meant for simple validation. Moreover, the same simplified cross-section of the excavation pit was used as in the previous PLAXIS 2D calculations. The input values for the calculations were based on the data in Table 4.1. The result of the hand-calculations is presented in Figure 4.7. For further explanation of the calculations, see Appendix B.

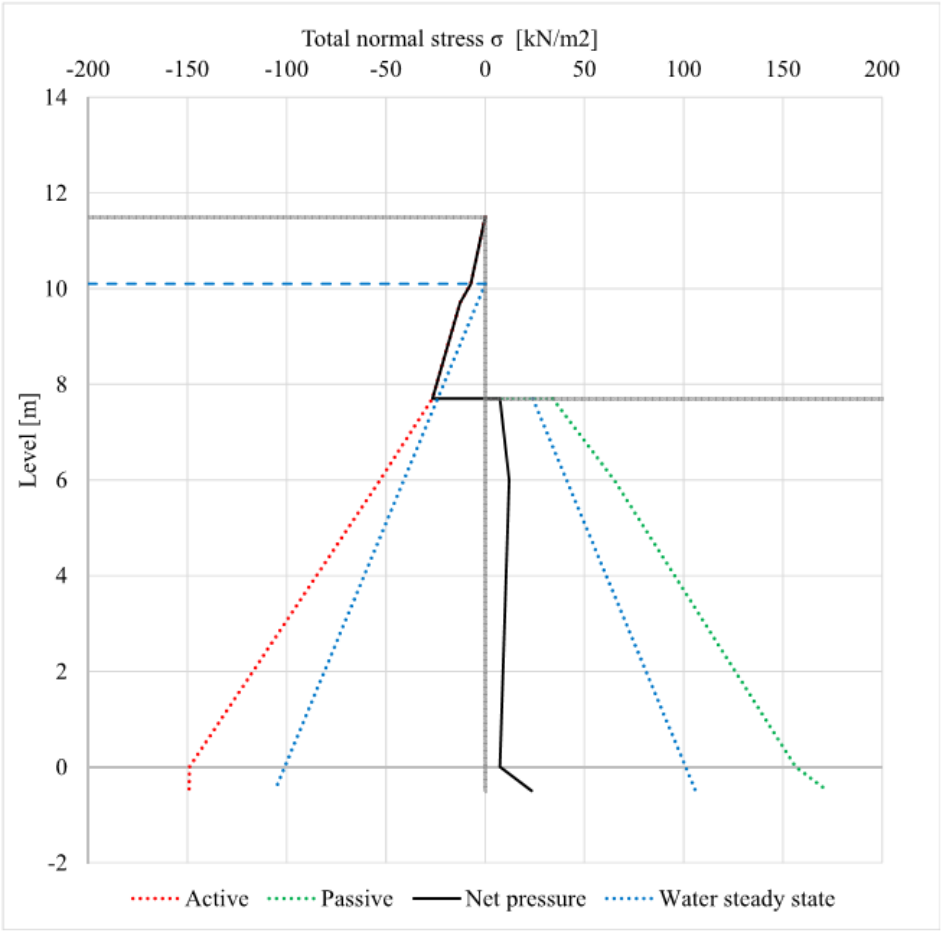

Figure 4.7 Lateral earth pressures, calculated by hand.

When comparing the results from PLAXIS 2D with the hand-calculations, it could be seen that the pattern of the lateral earth pressures on the wall were similar. However, the hand-calculated pressures in Figure 4.7 indicate that the net pressure is positive at the whole depth below the excavation, whereas the pressures generated in PLAXIS 2D in Figure 4.6 indicate that it becomes equal to zero kPa a few meters below the excavation. This was due to the level of simplicity in the hand-calculations.

Structure of the initial model

Since the results were similar, the structure of the excavation could be modelled more thoroughly. The modelled structure of the excavation was based on the description found in Chapter 4.1 combined with consultation meetings with Skanska Teknik, and can be seen in Figure 4.8. It should be noted that the casted concrete was set as a fixed-end anchor with a corresponding line load. This since heaving of the soil could result in a misleading horizontal force from the concrete. A small plate, with the same input values as for the sheet pile wall, was also modelled as connection for the prop and the anchor representing the concrete. The weight of the concrete slab was simulated as a line load of 2.4 kN/m. As mentioned in the construction description in Chapter 4.1, a surface load of 10 kN/m^2 was accounted for when the wall was designed. However, since the intention is to recreate the measured deformations, the surface load will not be taken into consideration.

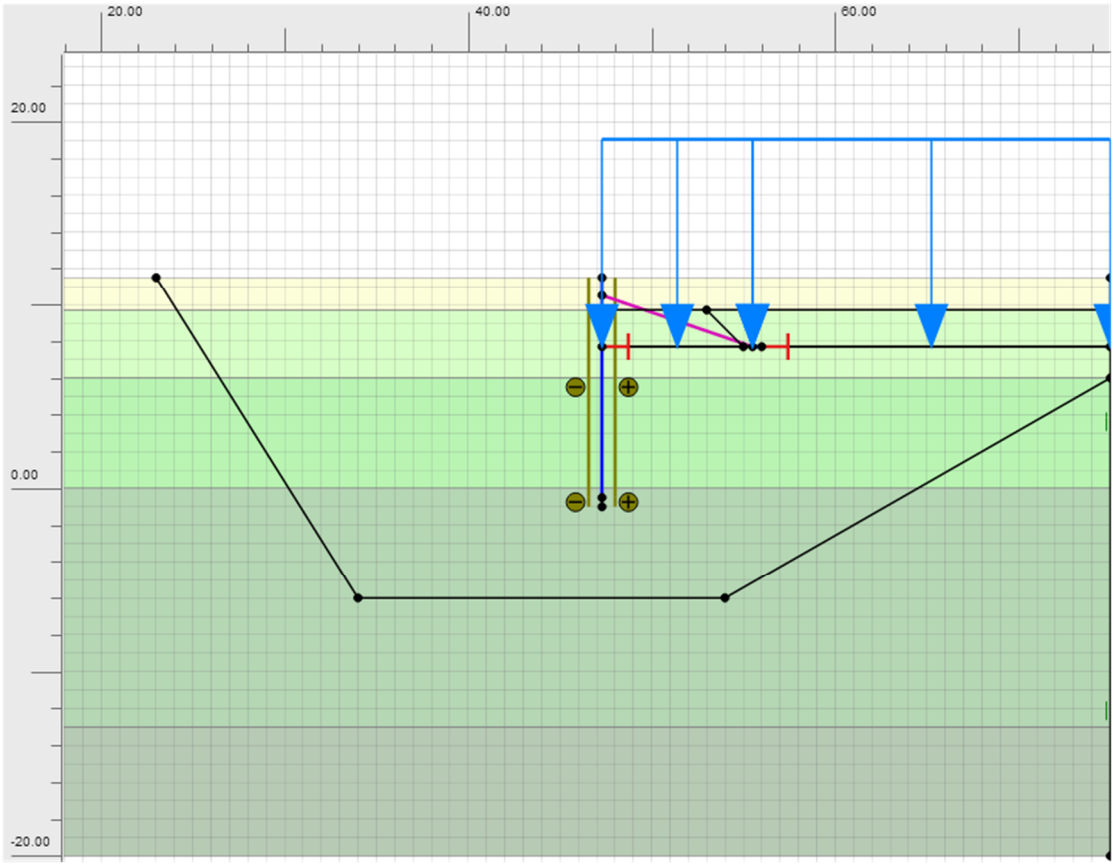

Figure 4.8 Structure of the initial model in PLAXIS 2D.

The parameters for the different structural elements can be seen in Tables 4.3 to 4.5. The values were set as input in PLAXIS 2D.

Table 4.3 Parameters for the sheet pile wall, type PU12 (Kullingsjö, 2011c).

Name	**Parameter**		**Unit**
Material type		Elastoplastic	
Normal stiffness	*EA*	2.94×10^{6}	[kN/m]
Flexural rigidity	*EI*	45.36×10^{3}	[kNm^2/m]
Weight	*w*	1.099	[kN/m/m]
Poisson's ratio	*v*	0	[-]

Table 4.4 Parameters for the concrete slab, type C25/30 (Kullingsjö, 2011c).

Name	**Parameter**		**Unit**
Material type		Elastic	
Normal stiffness	*EA*	3×10^{6}	[kN/m]
Length spacing	*L*	1.0	[m]

Table 4.5 Parameters for the prop, type HEB300-s355 (Kullingsjö, 2011c).

Name	**Parameter**		**Unit**
Material type		Elastic	
Normal stiffness	*EA*	3.131×10^{6}	[kN/m]
Length spacing	*L*	6	[m]

After this cross-section had been modelled, it was compared to an older version of the Tennet 2 model in PLAXIS 2D, simulated by Kullingsjö (2011c) at Skanska Teknik. This model was thought to be modelled correctly. It was found that the two models were similar regarding the design and structural elements, and the model was therefore found to be suitable for further analyses.

4.4 Creating the 2.5D-model

Since the initial model was similar to the one made by Kullingsjö (2011c) and as the hand-calculations indicated that the earth pressures were modelled correctly, it could be assumed that the created model was reliable enough for further investigation.

Setup of the 2.5D-model

Three cross-sections of the excavation, connected with a node-to-node anchor, were created in PLAXIS 2D. These constituted the so-called 2.5D-model, see Figure 4.9. The boundaries between the cross-sections were defined by line displacements, which separated the soils and groundwater.

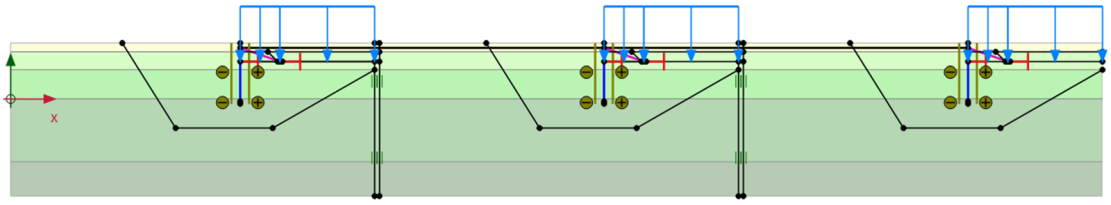

Figure 4.9 Structure of the 2.5D-model with three cross-sections.

The node-to-node anchor, connecting the cross-sections, was thought to simulate the wailing beam. The parameters for the wailing beam can be seen in Table 4.6.

Table 4.6 Initial parameters for the connecting wailing beam, type HEB300-s355 (Kullingsjö, 2011c).

Name	**Parameter**		**Unit**
Material type		Elastic	
Normal stiffness	*EA*	3.131×10^6	[kN/m]
Length spacing	*L*	6	[m]

According to A. Kullingsjö (consultation meeting, January 9, 2017), the three cross-sections that were connected represented different stages of the excavation procedure The idea behind this model was to illustrate the influence of the wailing beam along the sheet pile wall, by changing one cross-section at a time to cause a kind of domino effect. The phase setup in PLAXIS 2D can be seen in Table 4.7 below, where phase 6 to 12 represent the staged excavation. The duration of each phase was based on consultation with M. Johansson (personal communication, March 14, 2017) and notes from the period of the construction. This was done as carefully as possible to facilitate for comparison of the real deformations. However, the notes were in some cases inadequate, which lead to interpolation of the dates. For example, the casting of the concrete towards the sheet pile wall should not take longer than one day, but because of the stated start date for the next staged excavation, the time for concrete casting was extended to two days. The duration of the phases should not affect the results when

performing a plastic deformation analysis, but may have a minor affect when simulating consolidation in PLAXIS 2D. Moreover, as described earlier, piles were installed soon after the excavation to the top level of the berm. The piles were not simulated in PLAXIS 2D since this project concerns the staged excavation. However, in order to fit the results in PLAXIS 2D with the measured deformations, the time frame for the installation of the piles was set as a phase in the simulation. The calculation type for this phase was set to plastic for both the plastic and consolidation analyses.

Tabell 4.7 Phase setup for the 2.5D-model. The numbers in the parentheses represents the total duration.

Phase	**Duration [days]**	**Cross-section**			
		All	1	2	3
1	2 (2)	Installation of the sheet pile wall, activation of surface load.			
2	9 (11)	Excavation to the top level of the berm.			
3	16 (27)	Waiting time for piling.			
4	10 (37)	Excavation in the centre to the final depth.			
5	11 (48)	Casting of coarse concrete in the centre of the excavation.			
6	11 (59)	Installation of wailing beam and props			
7	3 (62)		Excavation of the berm		
8	2 (64)		Casting of concrete		

			against the retaining wall		
9	3 (67)			Excavation of the berm	
10	2 (69)			Casting of concrete against the retaining wall	
11	3 (72)				Excavation of the berm
12	2 (74)				Casting of concrete against the retaining wall
13	5 (79)	Removing props			

Simulation with the initial 2.5D-model

In PLAXIS 2D, it was chosen to use 15 nodes for the model. The mesh was refined close to the excavation and coarsened at distance. When evaluating whether to use medium or fine as general setting for the mesh generation, both alternatives were tested and the results were compared in terms of total displacement. It was found that when using a fine mesh, the difference compared to the medium mesh was significantly less than 10%. With this in mind, medium mesh was chosen since the computational time would decrease.

For comparison of the measured deformations of the sheet pile wall, one node on each sheet pile wall was evaluated, located at the level of the wailing beam. After the first calculation, the horizontal deformations of the sheet pile wall were evaluated. It was seen that the deformation patterns were somewhat similar to the measured horizontal deformations until day 59, even though the values in PLAXIS 2D were higher, see Figure 4.10. After this, the deformations of the sheet pile wall in PLAXIS 2D behaved different compared to the measured deformations. It can be seen that the sheet pile wall was only deformed when the berm in the same cross-section was excavated because the nodes did not follow the same pattern compared to each other. If the excavation had been successfully modelled, the sheet pile wall should have been deformed independent on what berm being excavated. In addition, the modelled deformations increased drastically in the last phase, when the props were removed. This pattern could not be seen in the measured deformations. This indicated that the excavation was modelled correctly in PLAXIS 2D before the staged excavation had started and the wailing beam had been implemented. Because of this, the first 59 days were set aside when evaluating the effects of the simulated wailing beam for further improvements.

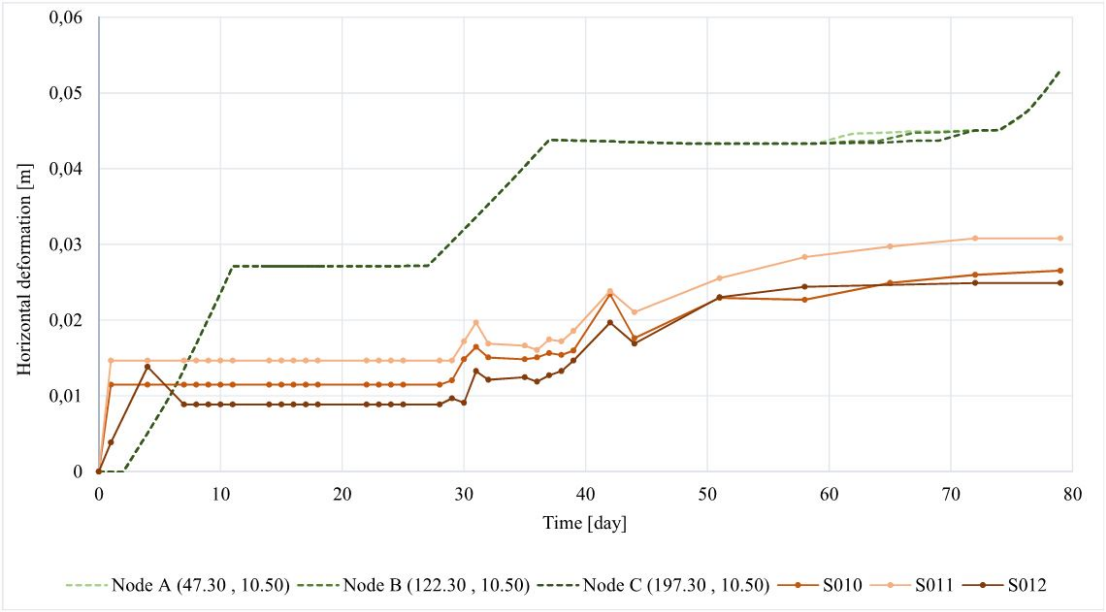

Figure 4.10 Horizontal deformation of the sheet pile wall at the level of the wailing beam, modelling with the initial 2.5D-model.

It was tested to deactivate the wailing beam and compare the deformations to the previous results, see Figure 4.11. Note that in this figure, only the simulated deformations during the last 29 days are shown. It can be seen that there was almost no change in the deformation patterns nor in the final deformations if the wailing beam was removed from the model. In other words, there was little effect from the wailing beam and the input parameters for this element should be further analysed.

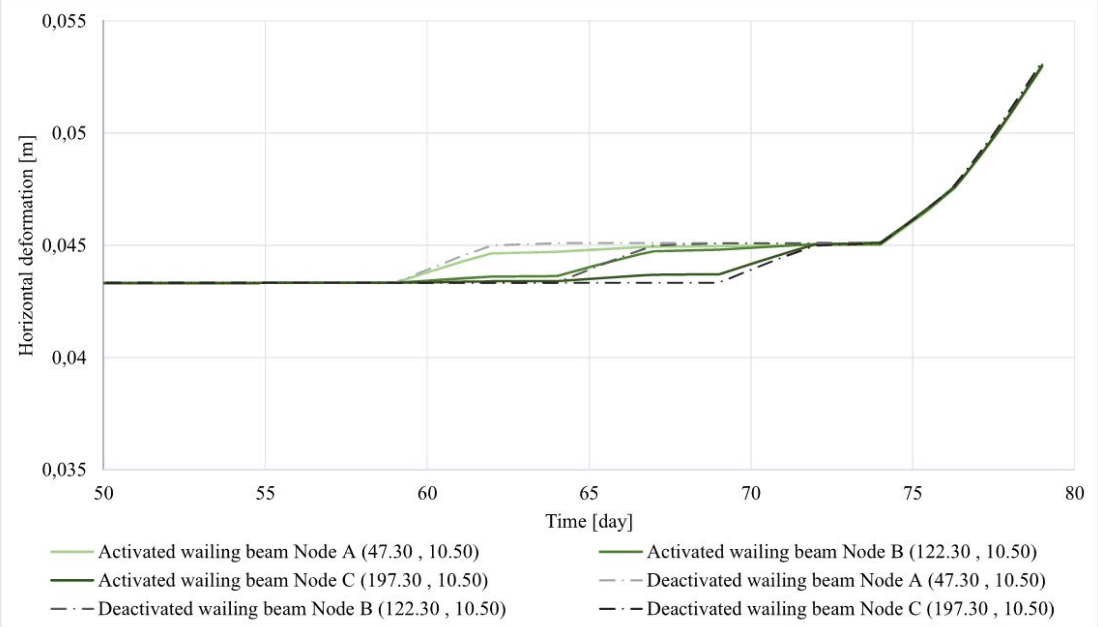

Figure 4.11 Horizontal deformation of the sheet pile wall, when deactivating the wailing beam.

Simulation with stiffer wailing beam

Since there was little effect from the wailing beam, it was tested to increase the stiffness, *EA*, of the wailing beam by 10^{10} kN/m. This caused for the deformations at the nodes to be the same at the same time, see Figure 4.12. This was a more logic pattern since the evaluated nodes were, as mentioned before, placed at the same height as the stiff wailing beam, which should result in them having a similar deformation. However, the updated stiffness of the wailing beam was not realistic, but necessary to cause intercommunion between the cross-sections.

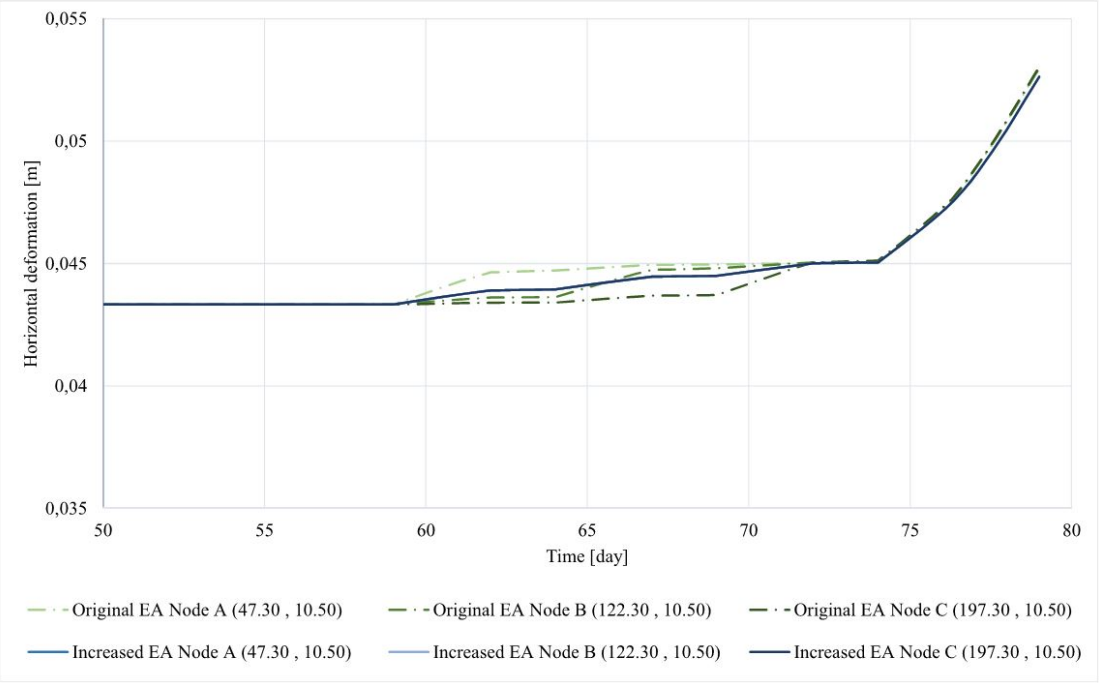

Figure 4.12 Horizontal deformation of the sheet pile wall, with increased stiffness of the wailing beam. Note that the three curves representing the increased stiffness are identical, why only one line is apparent.

The cross-sections now affected each other significantly more than in the previous models. However, the magnitude of the final deformations were still the same since the deformations still increased significantly at the last phase when the props were removed. In other words, the total deformation did not change if the wailing beam was deactivated or if it was made stiffer, but the deformation pattern did. It was concluded that this could be due to an error in the boundary definitions. Since the cross-sections only were anchored in each other, and no fix points were defined, the benefit of the wailing beam was as great as the disadvantage. Due to this, it was clear that the boundaries of the 2.5D-model had to be changed.

The two cross-sections on the sides of the model were updated by installing two additional fixed-end anchors, at the location of the wailing beam. These additional anchors were implemented in the same phase as the waling beam and props. The anchors were thought to function as extensions of the wailing beam, limiting the sheet pile walls ability to move. The input parameters for the fixed-end anchors were set to the same as for the updated wailing beam. However, this resulted in no deformations being generated at all after the installation of the anchors, which was unrealistic. After this analysis, it was concluded that an updated model was needed, in which the boundaries would be a hybrid of the earlier two models.

Simulation with additional cross-sections

A new model was created with two additional cross-sections, located at the sides of the previous model, see Figure 4.13. As for the first model, these additional cross-sections were connected to the others by extension of the already existing wailing beam, and the fixed-end anchors were neglected.

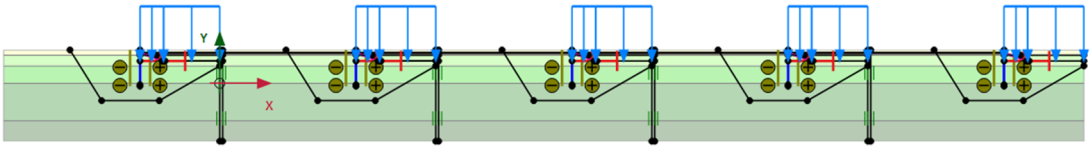

Figure 4.13 Structure of the 2.5D-model with five cross-sections.

The two new cross-sections were thought to function as the sides of the excavation in the real project. Looking at the construction notes and measured deformations, the corresponding berms at the sides of the excavation had not yet been removed at the final date of measuring. Due to this, in PLAXIS 2D, the berms in these two new cross-sections were set to be present for all phases, and no coarse concrete was casted against the sheet pile wall. The phase set-up were the same for the two new cross-sections as for the others during phase 1 to 5, see Table 4.7. However, in contrary of the pre-existing cross-sections, there was no change in the added cross-sections after phase 5. It was found that the deformation pattern was satisfying and that the total deformations now were reduced compared to the first model, see Figure 4.14. It can be seen that the deformations were influenced by the strength of the nearby retaining walls where there had been no excavation yet, which was especially noticeable during the last phase when the props were removed.

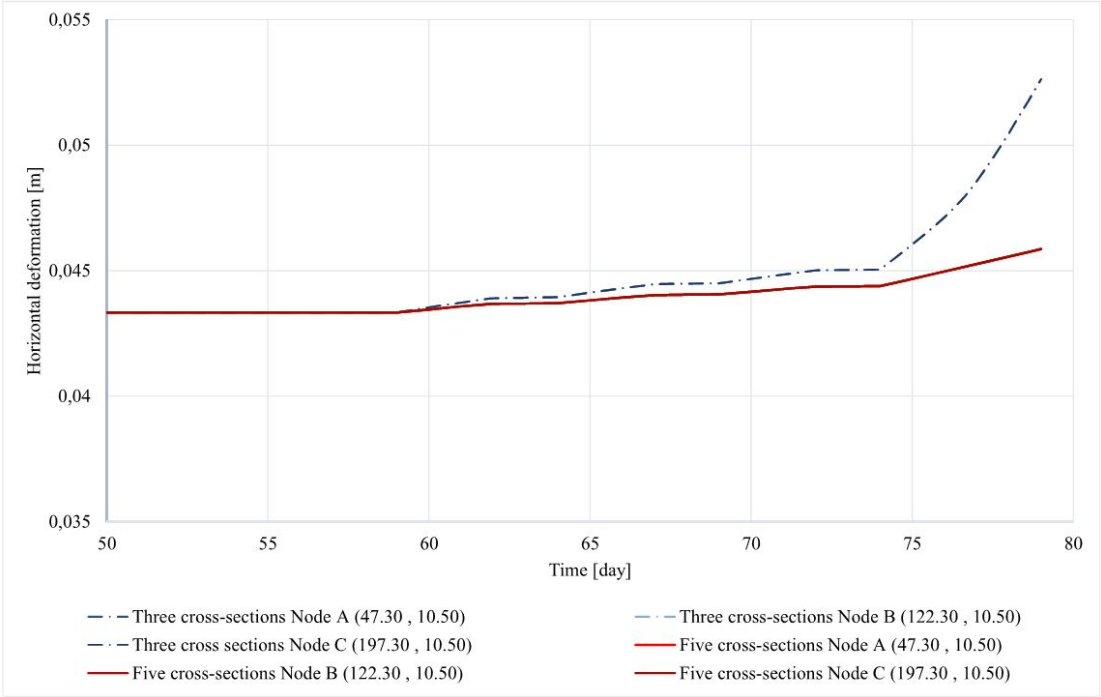

Figure 4.14 Horizontal deformation of the sheet pile wall, modelling with five cross-sections. Note that the nodes now follow the same pattern, why only two lines are apparent.

After these analyses had been performed, it was concluded that it would have been possible to model the excavation with just three cross-sections as well. If doing so, it should just be the middle cross-section being changed after phase 5, and the other two should simulate the unchanged ends of the excavation pit. However, the interconnection of five cross-sections facilitated for comparison with the measured deformations, and the effect of the wailing beam became more apparent.

Validation of horizontal deformations

Due to the duration of the phases in PLAXIS 2D not being fully on point compared to the stage duration during the real excavation, there were some minor differences in the deformation patterns. However, clear resemblance between the simulated and measured deformations was found. Moreover, it was found that the simulated deformations were linear, which is one of the drawbacks with the Mohr-Coulomb model since it assumes perfectly-plastic behaviour in the soil. In addition, the simulated deformations were approximately twice as great compared with the measured ones.

As mentioned before, the unloading modulus can be empirically derived by using either equation 4.1 or 4.2. Depending on what factor being used, equation 4.2 could result in two different modules, see Table 4.8. In Table 4.8, *Initial* represents the estimation of the unloading modulus, used during the real project, see equation 4.1. *Alternative 1* and *2* represent the modules retrieved if using equation 4.2. The values of the preconsolidation stress, σ_c', were retrieved from Constant Rate of Strain (CRS) tests, see Appendix C. Note, for clay layer 1, no representative CRS test had been conducted, why the same values were used as for clay layer 2. The differences, shown in Table 4.8, show the difference in percentage for the two alternatives compared to the initial estimation.

Table 4.8 Variation of the unloading modulus, when using the Mohr-Coulomb model.

	Empirical estimation	Clay 1 (no CRS)	Clay 2 (CRS 9m)	Clay 3 (CRS 15m)	Clay 4 (CRS 25m)
Initial	$E_{ur} = 500c_u$	8500	8500	10500	18500
Alt. 1	$E_{ur} = 2 \cdot 50\sigma_c'$	5900	5900	9200	17500
Diff [%]		-30.6	-30.6	-12.4	-5.4
Alt. 2	$E_{ur} = 3 \cdot 50\sigma_c'$	8850	8850	13800	26250
Diff [%]		4.1	4.1	31.4	41.9

As can be seen in Table 4.8, the increase in stiffness by depth would have been more apparent if *Alternative 1* or *2* would have been used. In Figure 4.15, the resulting deformations of the sheet pile wall are presented, when modelling with both *Alternative 1* and *2* compared to the initial estimation. Due to the significant increase in stiffness, *Alternative 2* would have resulted in the greatness of the deformations to be more similar to the measured ones, while Alternative 1 would have resulted in a general decrease in stiffness.

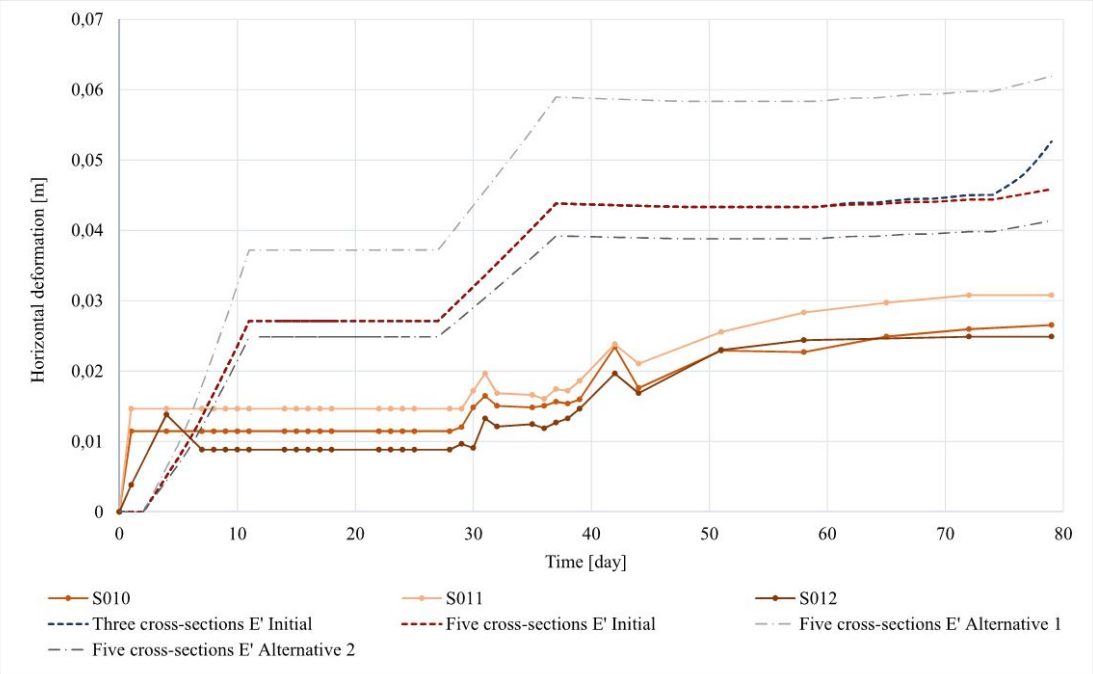

Figure 4.15 Horizontal deformation of the sheet pile wall when varying the unloading modulus.

Even though the deformations in Figure 4.15 are more similar to the measured ones when modelling the effective stiffness based on *Alternative 2*, the initial formula will be used for the stiffness in the further analyses. This because it was used during the project at Skanska Sverige AB by Kullingsjö (2011c), and because the initial values seem to be a sort of compromise between Alternative 1 and 2.

Validation of deformations by depth

To further validate the model, simulated deformations in the soil were compared to the measured deformations by the inclinometer K4. This was done by evaluating ten nodes by depth in PLAXIS 2D, one meter behind the sheet pile wall, see Figure 4.16. Once again, it was seen that the modelled deformations were greater than the measured, and that they were decreasing constantly by depth. The results registered by the inclinometer indicated that the deformations decreased drastically between approximately 7 and 15 meters depth, and that they were close to zero mm after 15 meters depth. However, the deformations generated in PLAXIS 2D decreased constantly from about 7 to 30.5 meter. It is of importance to remember that the five cross-sections, modelled in PLAXIS 2D, only were connected in one point via the wailing beam. In reality there are infinite numbers of interconnections, not only via the wailing beam but also via the sheet pile wall and the soil. Because of this, the level of accuracy in this 2.5D-model decreases when analysing nodes further away from the wailing beam connection.

The deformation pattern by depth was found to be the same for all dates, when modelling in PLAXIS 2D, see Figure 4.16. However, the measured deformations indicated that the pattern changed at the 6th of December. When evaluating the pattern at this date, the soil seemed to move more at two meters depth compared to the soil at the surface. This might have been due to disturbance of the inclinometer, or differences in the construction stages compared to the PLAXIS 2D simulations.

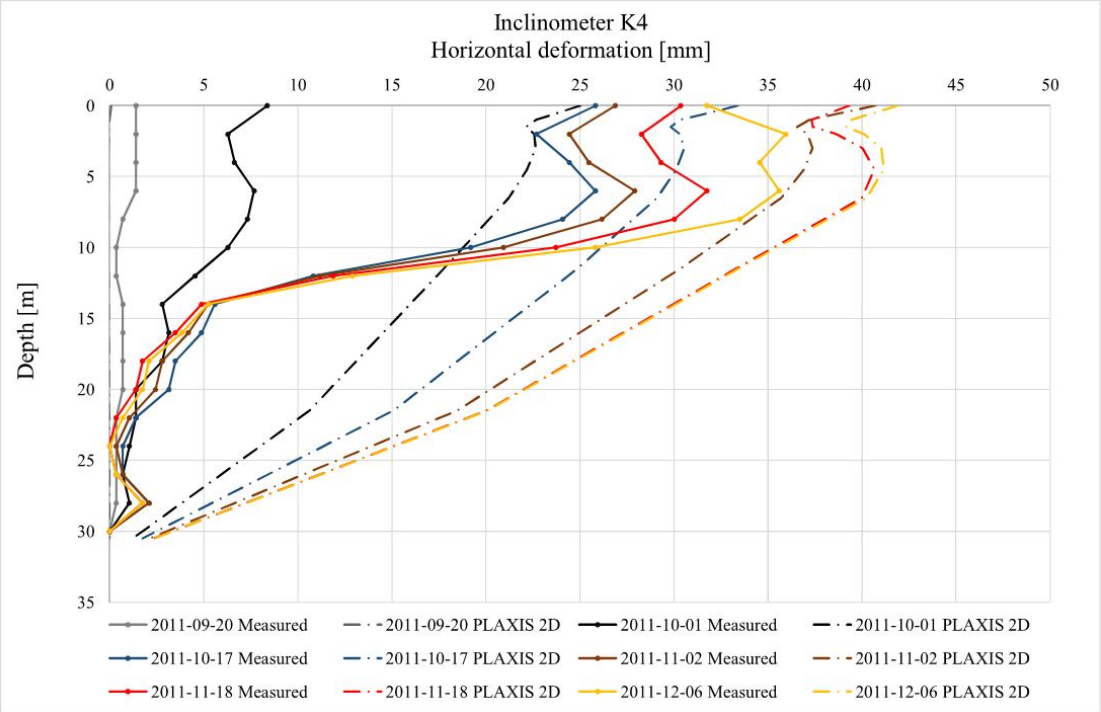

Figure 4.16 Deformations by depth behind the sheet pile wall, simulated with the 2.5D-model.

It can not be expected to retrieve the same magnitude of the deformation values, due to the drawbacks with Mohr-Coulomb and the fact that only one interconnection point was used. However, the deformation patterns generated in PLAXIS 2D, seen in Figures 4.15 and 4.16, were concluded to be sufficiently similar to the measured ones. With this in mind, the model was found to be designed properly, and it was decided to perform further analyses.

4.5 Input data Soft Soil model

In order to find the most suitable soil model for the 2.5D-model, further analyses involved modelling with the Soft Soil model. Because of this, it was necessary to derive the input parameters for this model. This was done by evaluating CRS-tests that had been performed for different depths in the area, see Appendix C. The values for the modified compression index, λ^*, and the modified swelling index, κ^*, were determined by the inclination of the normal compression lines in the CRS-tests. λ^* was calculated with the given value of the constant constrained modulus of the virgin compression line, M_L. Moreover, the value of the modified swelling index, κ^*, is dependent on the Unloading/Reloading modulus, M_{ur}. However, since there were no unloading in the CRS-tests, M_{ur} had to be estimated. According to A. Kullingsjö (consultation meeting, March 6, 2017) and Ismail and Teshome (2011), M_{ur} can be estimated according to equation 4.3

$$M_{ur} = (3\ to\ 6) \cdot M_0 \tag{4.3}$$

M_0 is the constant constraint modulus below effective vertical preconsolidation in the CRS-tests. κ^* can also be derived by the Unloading modulus, M_{ul}. According to

Persson (2004), this Unloading modulus, M_{ul}, can be estimated as a function of σ_c' and σ_v', see equation 4.4

$$M_{ul} = max \begin{bmatrix} 400\sigma_v' \\ 1500\sigma_c' \left(\frac{\sigma_v'}{\sigma_c'}\right)^4 \end{bmatrix} \tag{4.4}$$

However, due to the limited time, the estimation proposed by Persson (2004) was excluded for calculation of M_{ul} in this report. It was instead decided to estimate κ^* based on equation 4.3. The modified swelling index defines the stiffness of the soil, and a decreased value of κ^* increases the stiffness, why it was of interest to evaluate the range of M_{ur}, hence κ_1^* and κ_2^* in Table 4.9. The calculations done to derive κ^* and λ^* can be found in Appendix D.

Furthermore, by evaluating the ratio between the preconsolidation pressure and present effective stress, the overconsolidation ratio (OCR) was estimated according to equation 4.5 (Knappett & Craig, 2012)

$$OCR = \frac{\sigma_c'}{\sigma_v'} \tag{4.5}$$

The input parameters for the SS-model can be seen in Table 4.9. Each clay layer had representative results from the CRS-tests except for the first clay layer. This undefined clay layer was assumed to have the same values as for the layer beneath. The characteristics of the fill layer was set to be simulated with the Mohr-Coulomb model when using the Soft Soil model as well.

Table 4.9 Input data for the Soft Soil model Undrained (A) and Drained.

	Unit	Clay 1	Clay 2	Clay 3	Clay 4
Level		+9.7 / +6.0	+6.0 / +0.0	+0.0 / -13.0	-13.0 / -20.0
Material behaviour		Undrained (A) / Drained	Undrained (A) / Drained	Undrained (A) / Drained	Undrained (A) / Drained
γ	[kN/m^3]	15.5	16	16.5	16.5
ν_{ur}'	[-]	0.15	0.15	0.15	0.15
λ^*	[-]	0.096	0.096	0.168	0.221
κ_1^*	[-]	0.0210	0.0210	0.0150	0.0113
κ_2^*	[-]	0.0105	0.0105	0.0075	0.0056
c_{ref}'	[kN/m^2]	1.7	1.7	2.1	3.7
φ'	[^{o}]	30	30	30	30
ψ	[^{o}]	0	0	0	0
OCR	[-]	1.2	1.2	1.0	1.2

5 Evaluation of the constitutive models

After the setup of the model had been validated, the constitutive models Soft Soil and Mohr-Coulomb were evaluated and compared. In order to state which model being the most suitable for this kind of geotechnical problem, deformations of the sheet pile wall and resulting lateral earth pressures were analysed.

5.1 Deformation analysis

For further analyses of the modelled excavation, with the Mohr-Coulomb model, it was chosen to evaluate both Undrained (B) and (A). Moreover, consolidation analyses were performed to better understand the structural behaviour during the construction. After this, the same analyses were performed but with the constitutive Soft Soil model. This model was evaluated to see whether the pattern or magnitude of the calculated deformations could be improved and resemble the measured deformations more accurately.

5.1.1 Mohr-Coulomb model

When performing the plastic deformation analysis, using Undrained (A) with the Mohr-Coulomb model, the input parameters for the soil layers were set as seen in Table 4.2 in Chapter 4.2. The deformation pattern was found to be very similar to the previous results, but Undrained (A) resulted in slightly smaller deformations compared to when modelling with Undrained (B), see Figure 5.1. This indicated that the strength of the soil might have been slightly overestimated when performing the undrained analysis with effective strength parameters. The difference in deformation would probably have been even greater, between Undrained (A) and (B), if the soil would have been exposed to greater load, because then the total pore pressures would increase. This is something that should be taken into consideration if adding load during a safety analysis.

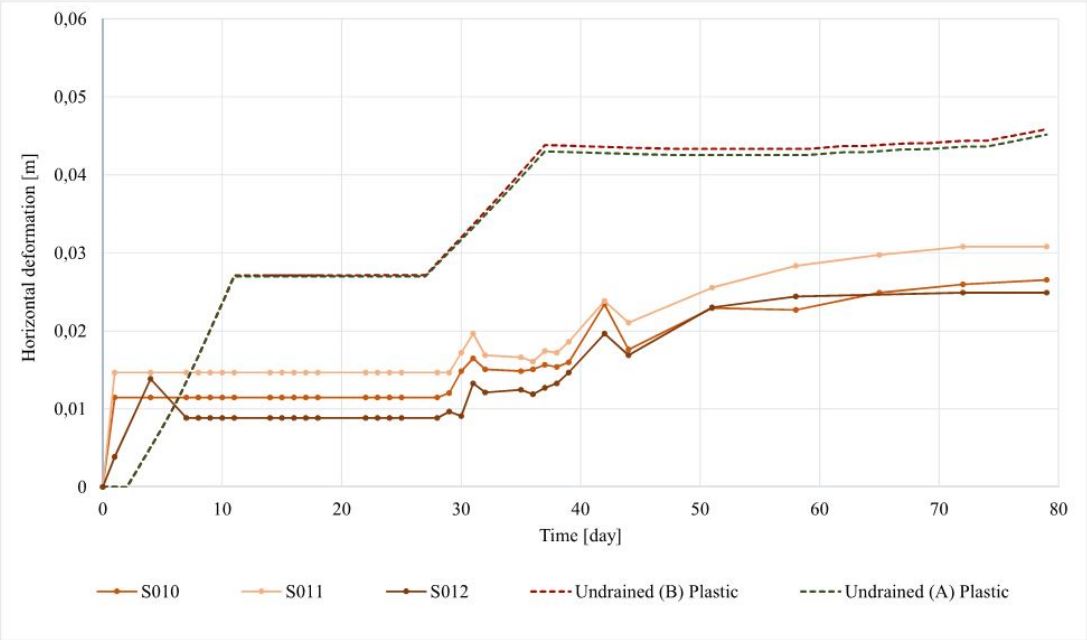

Figure 5.1 *Horizontal deformations of the sheet pile wall with plastic analysis using Mohr-Coulomb Undrained (A) and (B), compared to the measured deformations.*

After both Undrained (A) and (B) had been evaluated, the soil was simulated to be fully drained. This analysis was, like Undrained (A), based on effective stiffness and effective strength parameters. The calculations were however unable to succeed in PLAXIS 2D due to collapse in the soil. This was excepted since fully drained soil is the most critical condition for an excavation, and highly unlikely. Due to the collapse, it was decided to perform consolidation analyses for both Undrained (A) and (B). Although the Undrained (B) model is not suitable for consolidation analyses, it was of interest to evaluate how the deformations varied.

In order to perform the consolidation analyses, input data of the permeability in the soil layers was needed. The permeability, k, of the soil layers was based on the performed CRS-tests, and in PLAXIS 2D set according to Table 5.1 below. Note that the permeability of the fill layer was assumed to be one meter per day. Moreover, six nodes were used in PLAXIS 2D for the consolidation analyses since the models could not be simulated with fifteen nodes. This might have affected the accuracy of the results, which should be kept in mind when analysing the results.

Table 5.1 *Permeability of the soil layers.*

	Unit	Soil Layer				
		Fill	Clay 1	Clay 2	Clay 3	Clay 4
Permeability, k	[m/day]	1.00	1.81×10^{-4}	1.81×10^{-4}	9.50×10^{-5}	1.56×10^{-4}

In Figure 5.2, it can be seen that the deformations during the consolidation analyses were not that different compared to the plastic deformation analyses. This might have been due to the analyses being performed for an excavation and not an embankment. The Mohr-Coulomb model's drawbacks, concerning pore pressure generation, might not have affected the stress analyses as much as it would have done if the soil instead was exposed to a substantial load. However, it should be noted that drainage type (A)

generated greater deformations compared to (B), but vice versa for the plastic deformation analyses. This stresses the fact that Undrained (B) is not suitable for consolidation analyses, which was expected. After confirming this, Undrained (B) was neglected when performing consolidation analyses for further evolution.

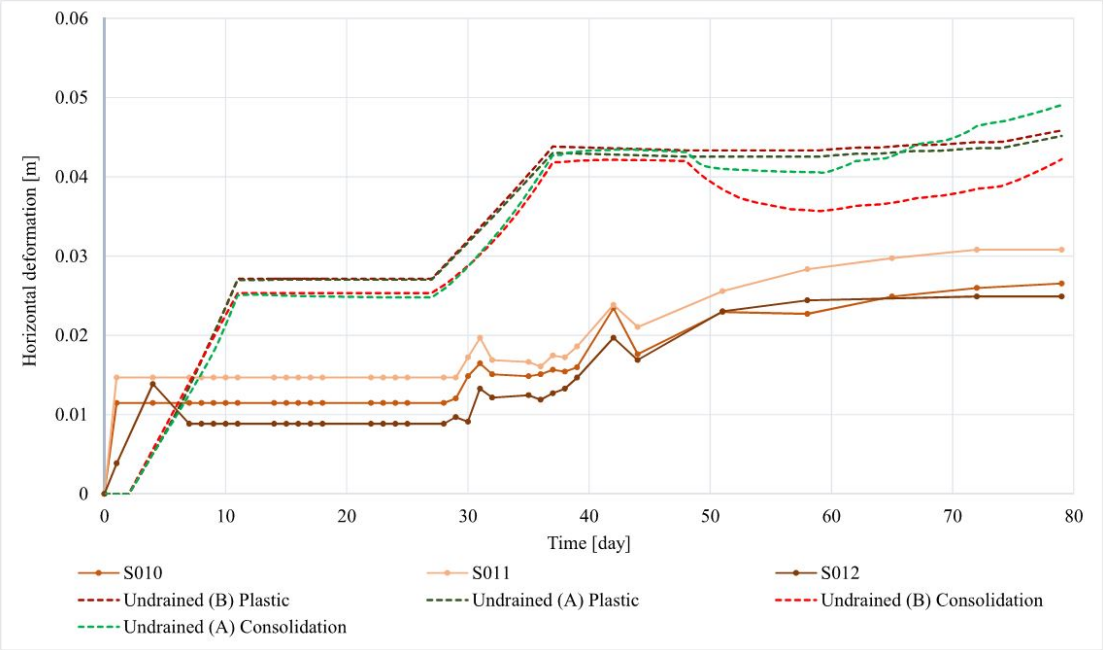

Figure 5.2 Horizontal deformations of the sheet pile wall with plastic and consolidation analysis using Mohr-Coulomb Undrained (A) and (B).

5.1.2 Soft Soil model

The deformation analysis with the Soft Soil model Undrained (A) was based on the input parameters from Table 4.9 in Chapter 4.5. When simulating with the Soft Soil model it could be seen that the deformations increased compared to the Mohr-Coulomb model, see Figure 5.3. The plastic simulation in the Soft Soil model, with κ_1^*, resulted in deformations being approximately twice as great as the measured. However, since the maximum number of iterations was exceeded in PLAXIS 2D, it was not possible to compute a consolidation analysis. In order to lighten the computational time, the drained interface parameters were changed to the input used in the previous Mohr-Coulomb simulations. A new plastic deformation analysis was therefore also performed, which resulted in 22 mm less deformation compared to when using the Soft Soil model to describe the interfaces, see Figure 5.3.

When comparing the consolidation and plastic deformation analysis, it was found that the correlation was similar to when modelling with the Mohr-Coulomb model. The consolidation analyses resulted in slightly greater deformations, and the staged excavation pattern was more apparent. As mentioned in Chapter 4.5, two different values for κ^* were evaluated; the greater value κ_1^* and the lower value κ_2^*. In Figure 5.3, it can be seen that the possible variation of κ^* highly affected the results, as there is a great range in deformation. By using one of the other methods for determination of κ^*, seen in Chapter 4.5, it is possible that more accurate results could have been received.

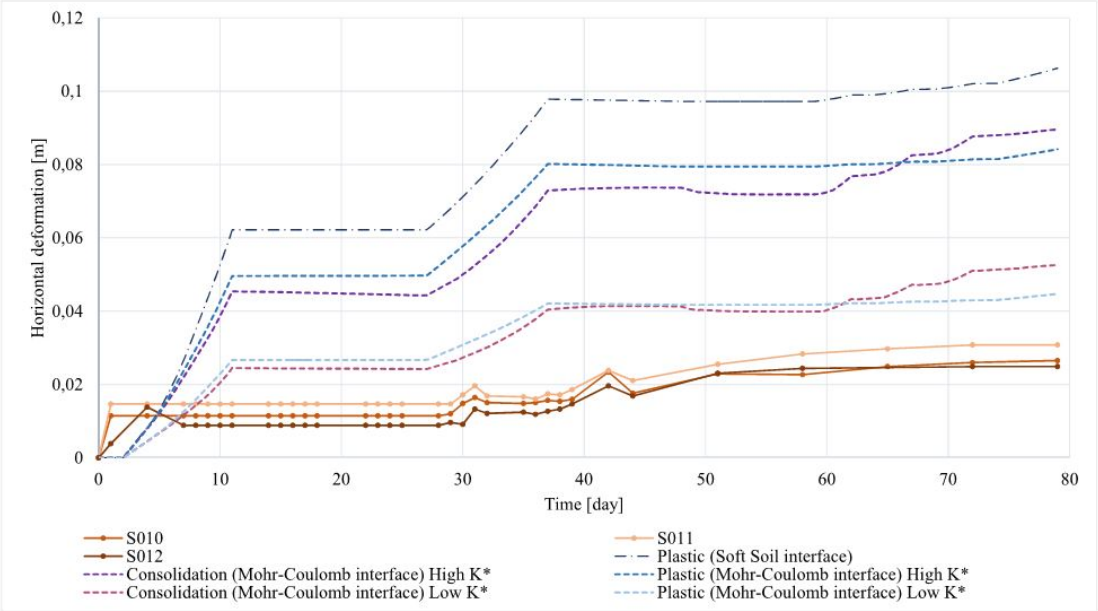

Figure 5.3 Horizontal deformations of the sheet pile wall with plastic and consolidation analysis using Soft Soil Undrained (A) with two different values of κ^*.

Since the low values of κ^* initiated lower deformations, it could be assumed to be the most accurate. Therefore, the values of κ_2^* were used for the further analyses.

5.2 Earth pressure analysis

In this section, analyses concerning the variation of earth pressure generation on the sheet pile wall are presented. This was done to find possible differences between the constitutive models, and not to spot weaknesses in the 2.5D-model. Due to previous findings, the lower values of the modified swelling index, κ_2^*, were used when modelling with the Soft Soil model to evaluate the earth pressures. Moreover, as mentioned before, the drainage type Undrained (A) was used for the consolidation analysis with the Mohr-Coulomb model due to the unsuitability with Undrained (B).

5.2.1 Mohr-Coulomb model

In order to validate the results using the different Mohr-Coulomb models, the earth pressures on the sheet pile wall at the last phase were compared. Looking at Figure 5.4 and 5.5, it can be seen that there were almost no difference in earth pressure generation between Undrained (A) and (B). Moreover, it can be seen that the net earth pressures were close to zero kN/m^2 below the bottom of the excavation at this stage. This indicated that the rotation of the sheet pile wall was almost fully counteracted by the wailing beam and props. At the last phase when modelling plastic deformation with drainage type (A), the factor of safety was found to be 2.53. However, it should be kept in mind that no partial coefficients were used during the analyses in this report, why it looks like the wall is overdimensioned. In order to validate the length of the sheet pile wall, back-calculation of the factor of safety was performed, see Appendix E.

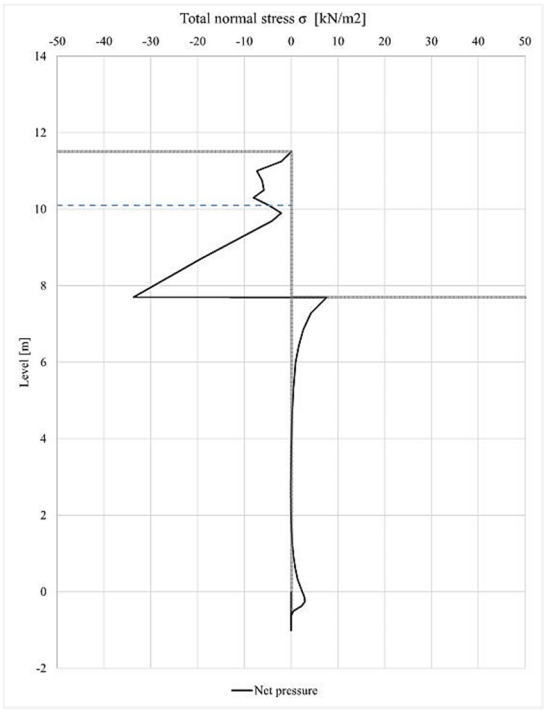

Figure 5.4 Lateral earth pressure when using the Mohr-Coulomb model Undrained (B), plastic analysis.

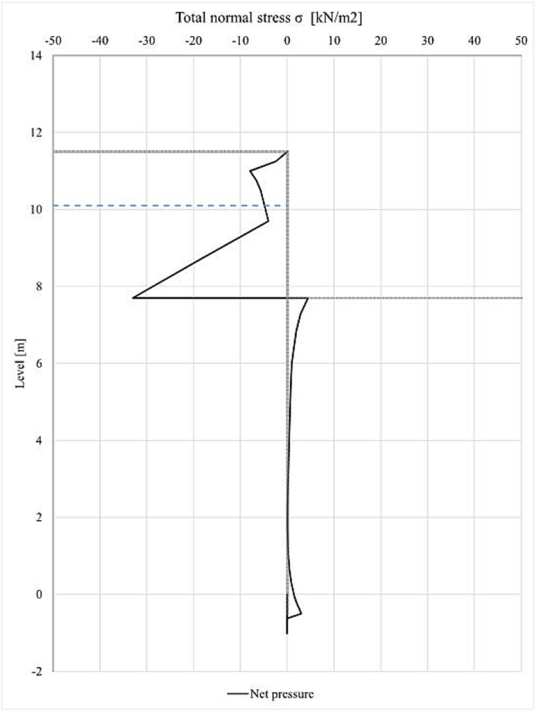

Figure 5.5 Lateral earth pressure when using the Mohr-Coulomb model Undrained (A), plastic analysis.

The pressures looked a bit different when performing the consolidation analyses compared to the plastic deformation analyses, see Figure 5.6. It can be seen that the pressures were slightly greater during the consolidation analyses. This indicated that the sheet pile wall was less stable during consolidation compared to the plastic deformation analyses, which was expected. Moreover, when looking at the earth pressure generated during consolidation, using drainage type Undrained (A), it was found that the passive earth pressure did not have a constant increase. Instead, the net pressure had a zigzag pattern below the bottom of the excavation. This was most likely due to numerical instabilities and differences in pore pressure generation compared to plastic analysis. The pattern might have been different if an even finer mesh would have been set at this level.

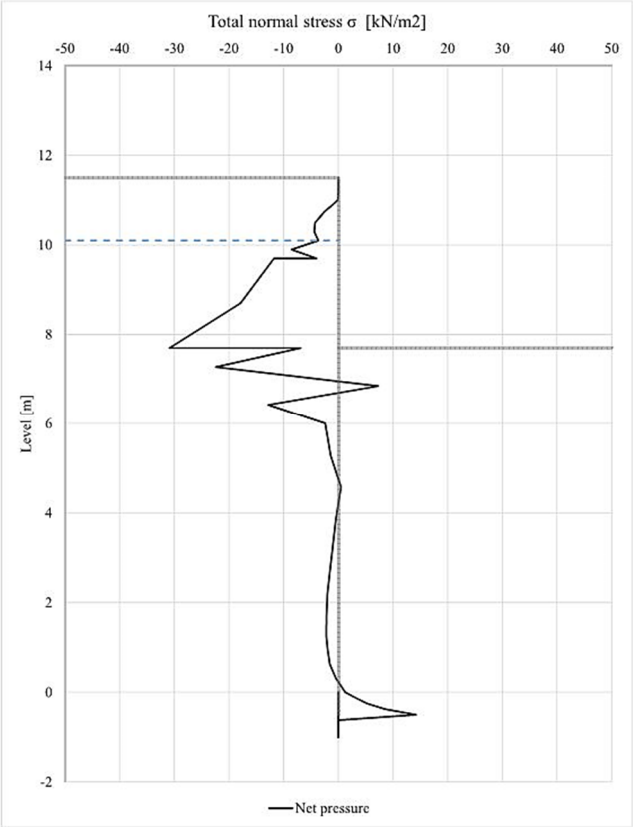

Figure 5.6 Lateral earth pressure when using the Mohr-Coulomb model Undrained (A), consolidation analysis.

5.2.2 Soft Soil model

The earth pressures on the sheet pile wall during plastic deformation analysis, when modelling with the Soft Soil model, were found to be similar in magnitude to the ones generated with the Mohr-Coulomb model, see Figure 5.7. However, in contrast to the pressures generated with the Mohr-Coulomb model, it can be seen that the net pressure on the active side below the excavation at the last phase was slightly greater. Moreover, the factor of safety at this phase was found to be 2.31, which was about 9 % less compared to when modelling with the Mohr-Coulomb model. When studying the deformed mesh in PLAXIS 2D, the wall was being pushed instead of bending as when modelling with the Mohr-Coulomb model. This was most likely due to the stiffness in the soil not increasing as much by depth when modelling with the Mohr-Coulomb model compared to when modelling with the Soft Soil model. This is a result of the linear elastic perfectly-plastic deformations in the Mohr-Coulomb model. The Young's modulus, E', is not stress-dependent in the Mohr-Coulomb model. Instead, the increase of the stiffness modulus by depth was constant and set manually, which contributed to uncertainties in the calculations.

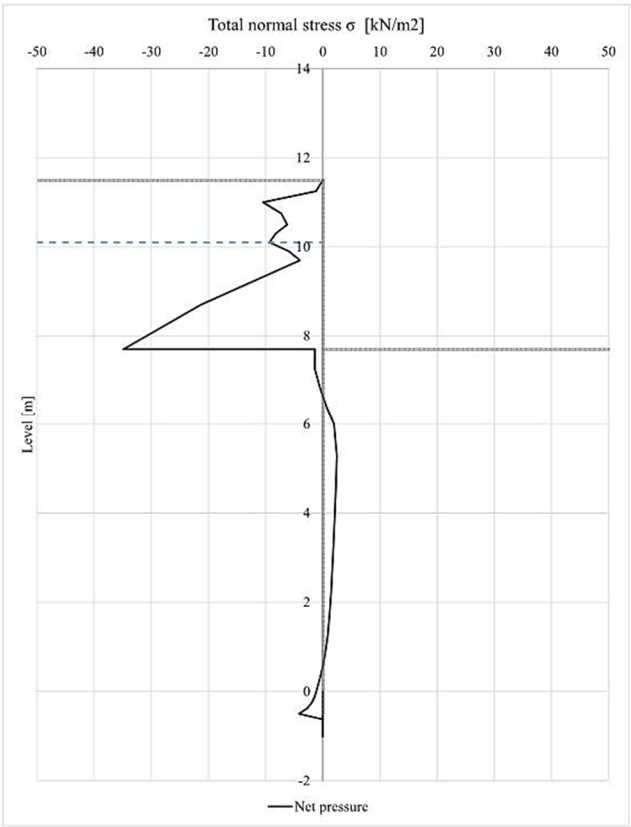

Figure 5.7 Lateral earth pressure when using the Soft Soil model Undrained (A), plastic analysis with κ_2^*.

When performing the consolidation analysis, the earth pressures were almost identical above the excavation bottom compared to when using the Mohr-Coulomb model, see Figure 5.8. Below the bottom, there was a small difference in the generated passive earth pressures. It can be seen that this resulted in the net pressure being slightly greater when modelling with the Soft Soil model. Furthermore, there was no significant difference in the net earth pressure when varying the values for κ^*, except from that the passive earth pressures slightly increased when κ^* was increased. This was expected since an increase in κ^* decreases the stiffness of the clay, which increases deformations.

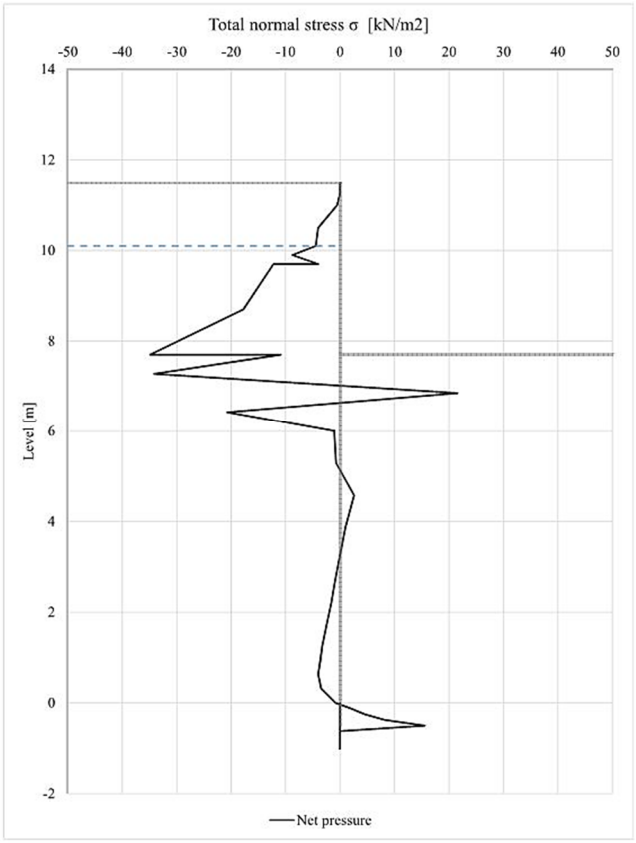

Figure 5.8 *Lateral earth pressure when using the Soft Soil model Undrained (A), consolidation analysis with κ_2^*.*

5.3 Comparison of deformations by depth

Looking at the net earth pressures, no model was distinctly more suitable for simulation of the staged excavation than the other. However, the consolidation analysis for Mohr-Coulomb Undrained (B) gave less deformation of the sheet pile wall than the plastic analysis which is not realistic, why it can be stated that Undrained (A) is more suitable.

Regarding the Soft Soil model, the reduced value of the modified swelling index, κ^*, resulted in deformations of the sheet pile wall which were closer to the measured. Since there was great uncertainties considering the value of κ^* before the simulations, it was assumed κ_2^* generated the most realistic results.

It should be mentioned that the deformations in a consolidation analysis increase with a longer time span, while the deformations generated during a plastic deformation analysis are not affected by the construction time. As could be seen in the results, this lead to the deformations in general being greater during consolidation compared to plastic deformation, why this analysis was found to be the most valuable. Moreover, the difference in deformation would probably have been even greater if the soil was subjected to great load. However, it should be kept in mind that the computational time increase significantly when performing the consolidation analyses. With this in mind, the consolidation analyses with the Mohr-Coulomb model Undrained (A) and the Soft Soil model Undrained (A) with the reduced value of the modified swelling index, were further evaluated regarding deformations by depth.

Figure 5.9 shows deformations by depth one meter behind the sheet pile wall, when modelling with the Mohr-Coulomb Undrained (A) compared to measured deformations, and Figure 5.10 shows deformations when modelling with the Soft Soil model. It can be seen that the deformations below the sheet pile wall, generated with the Soft Soil model, were more alike the measured. This pattern is a result of the automatically increased soil strength by depth. As mentioned before, in contrary to the Soft Soil model, the strength increase by depth had to be manually typed in when modelling with the Mohr-Coulomb model. This is a drawback with the Mohr-Coulomb model, and a too low strength increase might have been assumed during the modelling, why the deformations at the top were less compared to when modelling with the Soft Soil model, but greater at lower levels. The increase of the strength is assumed to be linearly increasing in the Mohr-Coulomb model, why also the deformations are linearly decreasing by depth, as seen in Figure 5.9.

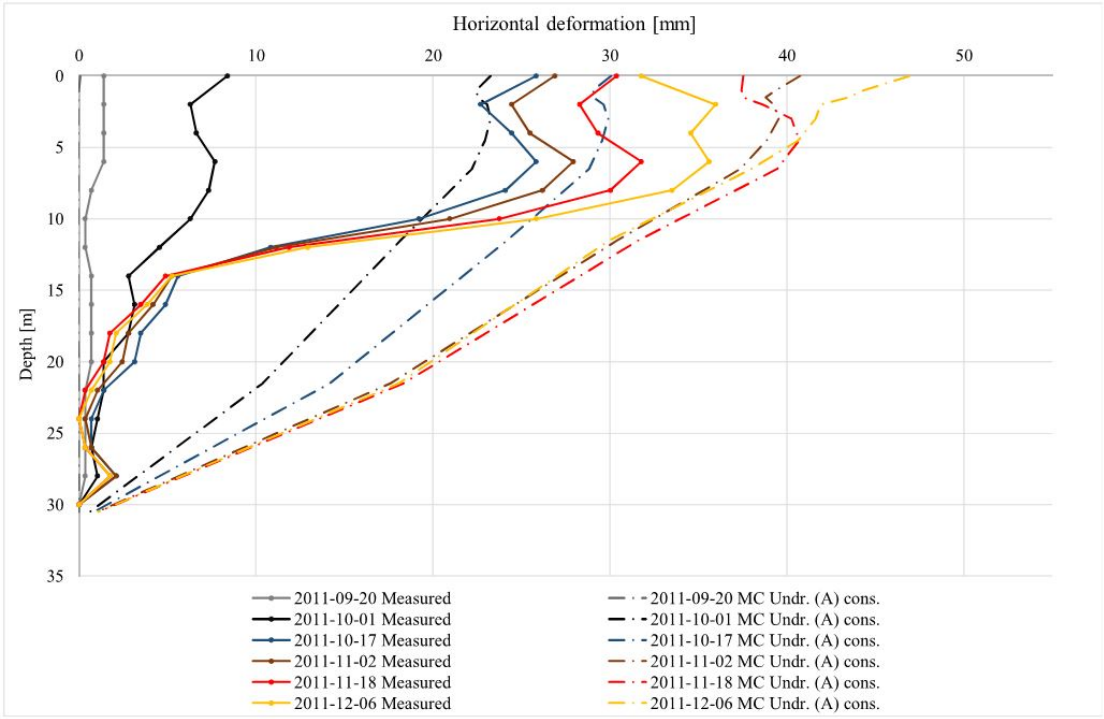

Figure 5.9 Deformations by depth when using the Mohr-Coulomb model Undrained (A), consolidation analysis.

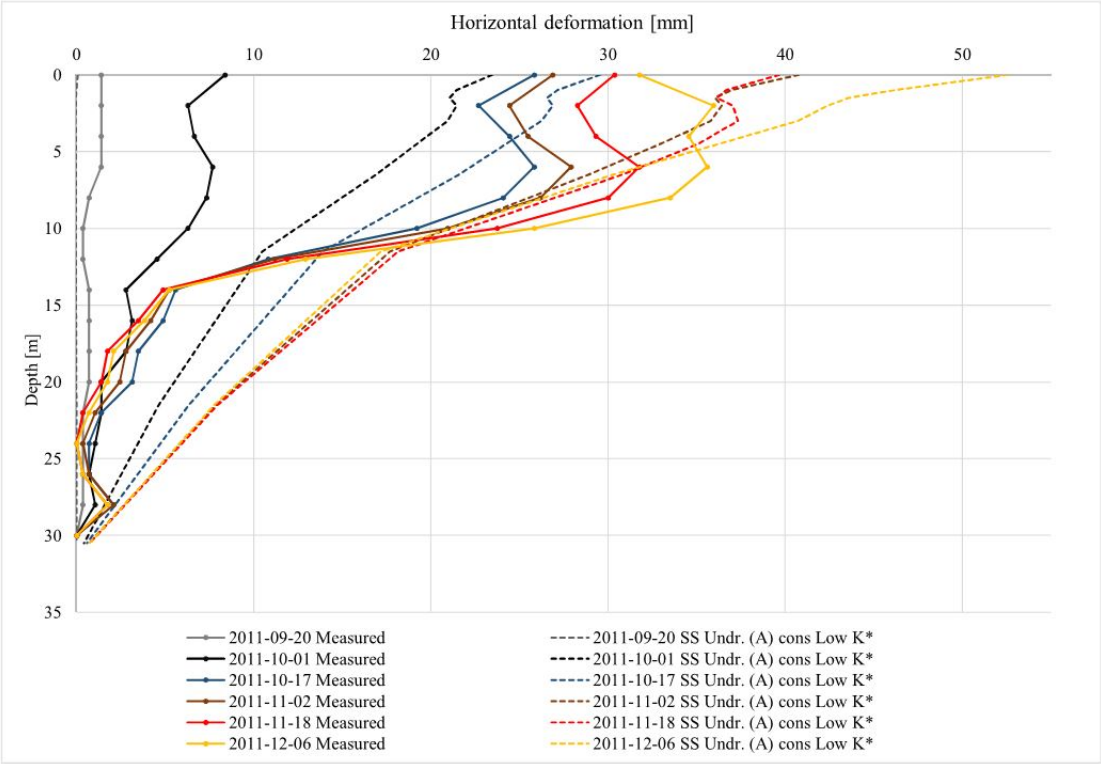

Figure 5.10 Deformations by depth when using the Soft Soil model Undrained (A), consolidation analysis with κ_2^*.

In Figure 5.11, the differences in deformation by depth, between the models, are shown. It can be seen that the magnitude in the generated deformations at the surface were much alike between the two models. However, at the 18th of November, the deformations at the surface increased when modelling with the Soft Soil model, compared to the Mohr-Coulomb model. At this date, the first berm is removed in the PLAXIS 2D calculations, which increases the forces in the wailing beam and prop. When looking at the figure, it becomes obvious that the net deformations increase by depth.

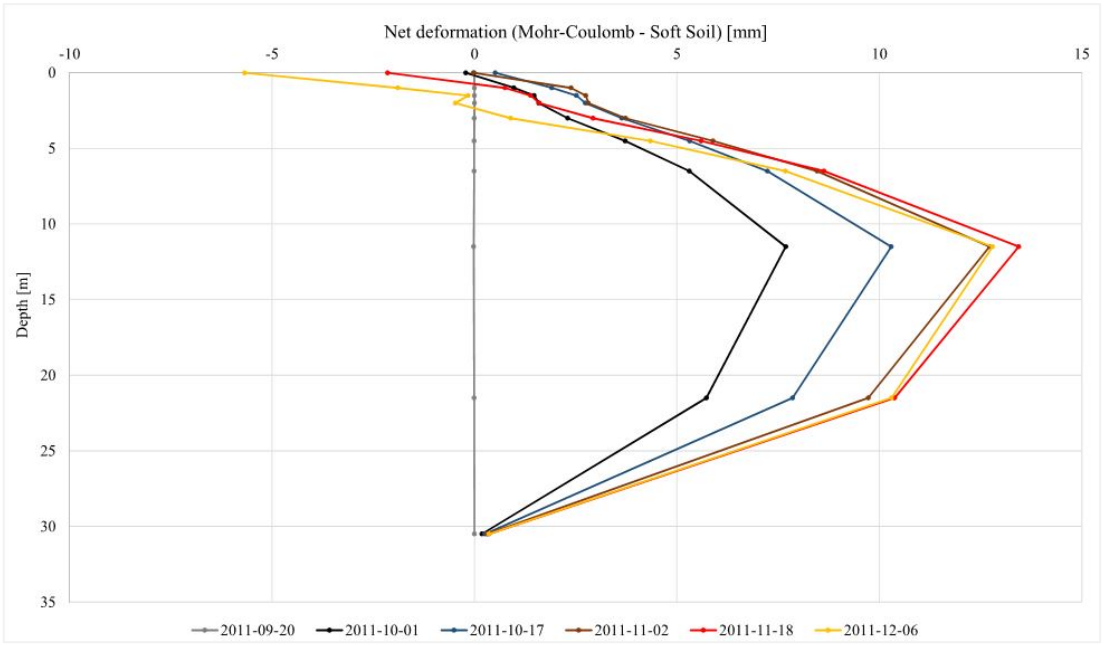

Figure 5.11 *Net deformations calculated as the Mohr-Coulomb minus the Soft Soil deformations.*

In Figure 5.12, the deformations of the sheet pile wall at the level of the wailing beam, are compared between the two models. The comparison in this figure correlated well with the resulting deformations by depth. It was found that before the excavation of the first berm, the deformations generated by the Mohr-Coulomb model were greater than with the Soft Soil model. After this, when the staged excavation starts at 62 days, the domino-effect is more apparent when modelling with Soft Soil, which contributes to the total deformations being greater compared to when modelling with the Mohr-Coulomb model. This indicates that the Soft Soil model was more sensitive to unloading compared to the MC-model.

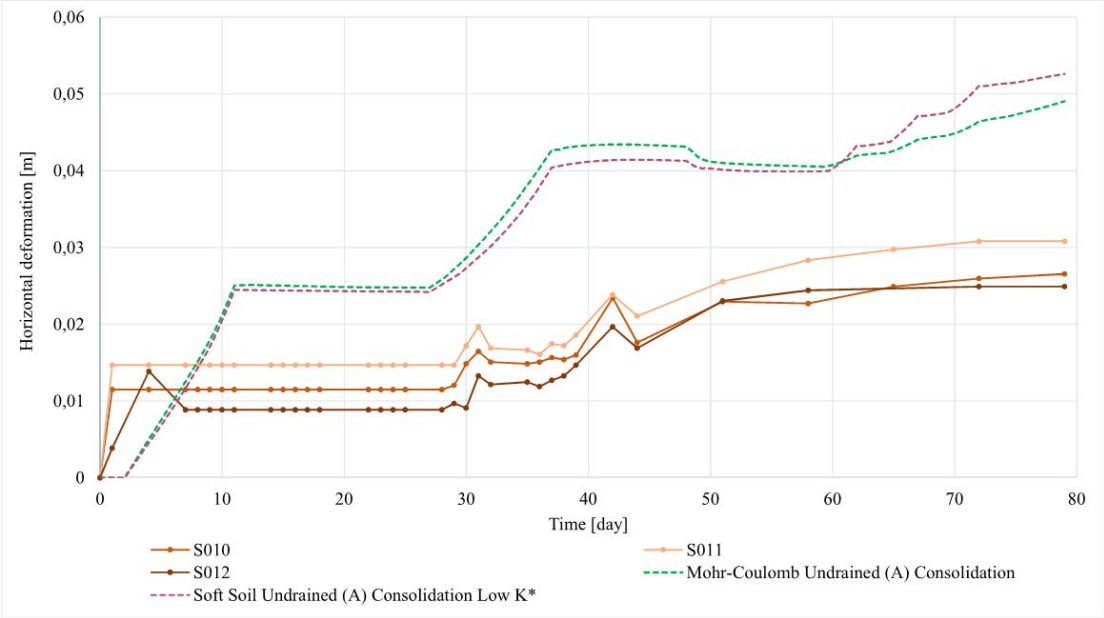

Figure 5.12 *Comparison between the models of deformations of the sheet pile wall at the level of the wailing beam.*

These results further indicate that the soil is more stiff at the surface in the Mohr-Coulomb model, compared to when modelling with the Soft Soil model. However, the stiffness increases more by depth, when modelling with the Soft Soil model, which could be seen in Figure 5.11. Thus, when modelling with the Mohr-Coulomb model, the stiffness is relatively great but the increase by depth is not as apparent. As mentioned before, this resulted in the wall being pushed forward. The stiffness is lower at the surface when modelling with Soft Soil, but increases more by depth, which contributes to the wall bending instead of being pushed. With this in mind, the most suitable model to use depends on the desired level to be studied.

6 Discussion

The aim of this project has been to create a model which should be able to simulate the staged excavation in conjunction with the project Tennet 2 in an effective and reliable way. In order to evaluate whether a 2.5D-model can be used, the procedure has been to perform back-calculations and to fit gathered data from the project. This has although been found to be difficult due to insufficient data regarding for example stiffness parameters from the real project. Moreover, the level of complexity in the 2.5D-model was not sufficient enough to fully recreate the behaviour of the soil in three dimensions, which lead to differences in the PLAXIS 2D calculations compared to the measured deformations.

6.1 Result evaluation

In the 2.5D-model, the only connection between the cross-sections was the wailing beam. Since there was only one connection point, the intended effect from the other cross-sections was limited and became very local. Since the wailing beam had not yet been activated during first two excavation phases, no benefit was generated from the more stable additional cross-sections. It can be stated that the 2.5D-model would have benefitted from implementing more connection lines, possibly simulating the rigidity of the wall or the shear strength of the soil. If the soil is divided into several partial areas, it would be possible to simulate the resultants of the shear strength for each area. The effect of the 2.5D-model would then have been apparent during the whole construction time. The idea with this project was however to create a simple model which would not require too much computational time, why it was thought that the produced 2.5D-model was sufficient enough.

After creating the structure of the 2.5D-model, the intention was to determine which of the Mohr-Coulomb and the Soft Soil models that resulted in deformations most alike the measured ones when using the 2.5D-model. By running several versions of each constitutive model, where soil parameters and drainage types were varied, and comparing the results with measured data, it could be concluded which models that were the most suitable for simulation of deformation behaviour. It was seen that the deformations, generated in PLAXIS 2D, were in general much greater compared to the measured. However, after studying the results, the most feasible models for modelling of the staged excavation were found to be the consolidation analyses with the Mohr-Coulomb Undrained (A) and the Soft Soil model with a low value of the modified swelling index, κ^*. These models resulted in similar deformation patterns, but when studying the deformed mesh in PLAXIS 2D, it could be seen that the sheet pile wall rotated more when using the Soft Soil model, while it instead was pushed when modelling with Mohr-Coulomb. This could be due to the fact that the Soft Soil model automatically changes the stiffness when there is a change in stresses, which in contrast had to be manually set when modelling with the Mohr-Coulomb model. In order to estimate the stiffness, interpolation was made between each soil layer in PLAXIS 2D. This increase was set to be constant, which most likely is not the case in reality.

When evaluating the earth pressure diagrams in Chapter 5.2, it was seen that there were little difference when comparing the constitutive models. What could be stated though was that the lateral net earth pressure was slightly greater when using the Soft Soil model. This was expected since the soil stiffness was obviously lower at the surface

and more of the sheet pile wall was required. It was also seen that the net earth pressures simulated from the consolidation analyses had a random pattern below the excavation bottom. This could be due to computational errors in the excessive pore pressure generation, possible faults in the setup of the interfaces, or due to other numerical instabilities. However, consolidation analysis should not be disregarded when evaluating the earth pressures, but the model should instead be improved so that the plausible numerical instabilities are corrected. Moreover, it is possible that the differences between the constitutive models would have been greater if there would have been a substantial load at the excavation. As discussed in Chapter 5.1.1, it is likely that the Mohr-Coulomb Undrained (B) then would have generated more reliable results, since the drained soil parameters c' and φ' only were assumed for Undrained (A).

As is stated in Chapter 5.3, it is more suitable to use the Mohr-Coulomb model if the deformations close to surface are of concern, and the Soft Soil model is more suitable if the deformations by depth are of interest. Since the behaviour of the wall is of more concern than the deformations at great depth, it can be assumed that the Mohr-Coulomb model Undrained (A) with consolidation recreated the conditions and deformations at Tennet 2 in a more valuable way compared to the Soft Soil model. Another advantage with the Mohr-Coulomb model is that it requires less computational time. Furthermore, the lack of necessary data of the compression modulus for the Soft Soil model also supports this conclusion. However, if more accurate and reliable data would have been provided, it is possible that the consolidation analysis with the Soft Soil model would have been the most suitable. In the end, everything comes down to the rough assumptions and it is difficult to definitely state which model that is the best.

By increasing the stiffness, the deformations could have become more similar to the measured. On the other hand, the stiffness set was already believed to be high for each soil layer. However, if the quality of the retrieved soil tests were to be improved, a more accurate setup of the stiffness would most likely be possible. This would likely enable for small strain analysis to be performed. With this in mind, the cause might have been that several minor uncertainties in the parameters combined were the reason for the inaccuracy. When modelling with the Mohr-Coulomb model, the stiffness modulus, E', was based on the unloading modulus, E_{ur}. However, E_{ur} was derived by assuming an empirical relationship to the undrained shear strength, c_{uk}. This resulted in the effective stiffness modulus being based on the undrained shear strength, which might have caused for the stiffness in the soil to be overestimated. When deriving the soil parameters for the Soft Soil model, one uncertainty was in the CRS-test at the depth of 9 meters where there was little difference in inclination between the elastic and plastic compression lines, defining the compression modules. This is not a realistic loading pattern, and might have been due to the test possibly being disturbed. If the elastic inclination would have been less, the value of κ^* would also have been reduced, resulting in a greater stiffness when modelling with the Soft Soil model. If this was corrected, the accuracy would most likely have been improved when comparing the results with the measured deformations.

6.2 Uncertainties and plausible key sources of error

Since the model was made in PLAXIS 2D, and excavations are in reality three-dimensional problems, several simplifications regarding the design had to be made when developing the model to 2.5 dimensions. For instance, it was found that the two additional end-cross-sections, simulating the sides of the excavation, were important.

The design of these were however uncertain as they in reality were perpendicular to the initial cross-sections. Moreover, the design of the wailing beam was completely based on the deformation patterns. Due to the high stiffness of the wailing beam, the perpendicular design, and the modelled length, it might be improper to compare it with the wailing beam from the project. It should instead be viewed as a connection line used when creating a 2.5D-model. However, due to the many previous assumptions and the time frame of this thesis, it was thought that an updated design would be out of the scope of this thesis.

Another drawback, with the 2.5D-model compared to when modelling in three dimensions, was the setup and modelling of the groundwater conditions. When the phreatic level was changed in one of the cross-sections, it did not affect the others in the 2.5D-model. Instead the groundwater conditions for the different clusters in PLAXIS 2D had to be manually changed. If the groundwater conditions were to be perfectly simulated, the earth pressures might have looked different.

The measured deformations presented in this thesis were difficult to match in PLAXIS 2D. It should be mentioned that there were uncertainties when evaluating the measured deformations registered at the Tennet 2 project. For example, the data of the measured deformations was corrected due to the piles that were installed after the first excavation. As was described earlier, the piles pushed the sheet pile wall away from the excavation, which resulted in negative displacements. It was however decided early in the modelling process that the piles would be neglected. This was a rough simplification, and the deformations in reality would probably have further increased without the piles. When simulating the period before the piling in PLAXIS 2D, the deformations were not time dependent which caused them to be greater than the measured ones. When viewing the generated deformations of the sheet pile wall in PLAXIS 2D, it can be seen that most of the deformations take place during this period of time. Therefore, if the piles would have been simulated in PLAXIS 2D, it is possible that the created 2.5D-model might have simulated more accurate deformations.

For this thesis, the deriving and evaluation of the soil parameters for the Soft Soil model required more contemplation compared to the Mohr-Coulomb model. This since the parameters for the Mohr-Coulomb model were retrieved from previous PLAXIS 2D calculations, performed by Kullingsjö (2011c) at Skanska Sverige AB. This lead to the impression of the parameters for the Mohr-Coulomb model being more reliable. However, it should be stated that these parameters were used for conservative and more simplified calculations regarding the dimensioning of the Tennet 2 excavation. The Mohr-Coulomb model is a common choice for a first impression of the resulting deformations. However, the fact that the model assumes the relation between the stress and deformations to be linear elastic perfectly-plastic, and overestimates the strength of the soil, makes the uncertainties of this model greater than the Soft Soil model.

Before the setup of the 2.5D-model, the importance and effects of the interface input data in PLAXIS 2D was relatively unknown. It became clear that the setup of the interfaces highly affected the results regarding strain. As mentioned in Chapter 5.1.2, the drained interface soil layers, when modelling with the Soft Soil model, were changed to be modelled with the Mohr-Coulomb model instead. This was done in order to lighten the computational time for the analyses. It was found that this measure decreased the deformations by roughly 21 % for the plastic analysis with the high value of κ^*, which indicated that the choice of model for modelling of the soil in connection to the structure highly affects the results.

6.3 Further investigations

The idea of the 2.5D-model was to create an efficient and precise simulation of a staged excavation. As seen in Chapter 4.4, the effect of the 2.5D-model reduced the deformations by 7 mm. The effect could probably have been even greater with the implementation of more connection lines. If the benefit of the shear strength in the soil could have been simulated by such connection lines, it would be possible to create an even more precise 2.5D-model. The effect of the 2.5D-model would then be apparent during all simulation phases. This would however require more advanced calculations, and it is possible that a simulation in PLAXIS 3D would be easier.

It was found to be difficult to create a fully reliable model due to the many uncertainties regarding soil parameters, construction notes, and structural design. For instance the soil stiffness, which normally is determined by evaluating unloading and reloading tests, had to be determined from empirical equations and CRS-tests in this thesis. If the 2.5D-model would be used in future projects, it is recommended to use data obtained from correct and reliable soil tests. Better and more realistic results that resemble the real deformation behaviour could then be simulated with the 2.5D-model. It should also be mentioned that there are several other constitutive models which have not been investigated in this thesis, some which might have simulated more accurate results. The modelling results should still be interpreted as quite conservative. Before viewing the model as basis for final decision making, its predictions should be validated by comparing it to a 3D-model.

If the 2.5D-model would be used in the design of a future staged excavation, it is possible that the design and construction costs could be reduced. However, as for now, the 2.5D-model is only affecting the results after the installation of the wailing beam. Until then, no benefit was generated from the more stable cross-sections in the ends, which only makes it useful if changes are to be made after the installation of the wailing beam. If the benefit from 2.5D-model could be implemented in an earlier construction phase, it is possible that the simulated deformations would be more accurate. A possible investigation could for example be regarding the variation of the size of the berms that are to be excavated. If this sort of investigation would have been potential during the design of the Tennet 2 excavation, it is possible that more of the berms could have been excavated during the same excavation phase. Evaluations like this could lead to reductions of the construction costs.

7 Conclusions

The aim of this thesis was to create a 2.5D-model that would in an effective and reliable way simulate the staged excavation in conjunction with the Tennet 2 project. This was found to be challenging due to the uncertainties regarding soil parameters and simplifications of the structure. The benefit of using additional cross-sections, to simulate the more stable ends of the excavation pit, was not present until the activation of the wailing beam. Still, the deformations were slightly decreased compared to when only using one cross-section, i.e. plain 2D. Furthermore, the defining of the interfaces were found to highly affect the results, why it is recommended to always check if the properties are sensitive to the interfaces.

The most significant difference between the constitutive models was the prediction of stiffness. This was due to that in contrast to the Mohr-Coulomb model, the Soft Soil model accounts for stress-dependency of the stiffness modulus. This means that the stiffness of the soil increases with pressure. Moreover, it was seen that all variations of the models generated greater deformations compared to the measured, whereas two versions were found to be more suitable than the others. It could be concluded that the consolidation analysis with the Mohr-Coulomb model, using the drainage type Undrained (A), simulated the most accurate deformations close to the surface. Consolidation analysis with the Soft Soil model, using Undrained (A) with the low values of the modified swelling index, κ^*, simulated better the deformations at greater depth.

If the 2.5D-model could be improved in a way that the positive contribution of the surrounding soil was simulated in PLAXIS 2D, the total deformations would decrease and the effect of the 2.5D-model would be apparent during the whole simulation process. If such an improved design of the 2.5D-model would be used in the design of a staged excavation, instead of plain 2D or 3D, there could be reduced design and construction costs.

8 References

Bartlett, S. F. (2010, 03 11): *Earth Pressure Thoery.* University of Utah, Salt Lake City.

Brinkgreve, R. B., & Shen, R. F. (2011): Structural Elements & Modelling Excavations in Plaxis. *[Power Point Presentation File].* Delf, the Netherlands.

Brinkgreve, R. B., Kumarswamy, S., & Swolfs, W. M. (2016a): *PLAXIS 2D 2016 Material Models.* The Netherlands: PLAXIS bv.

Brinkgreve, R. B., Kumarswamy, S., & Swolfs, W. M. (2016b): *PLAXIS 2D 2016 Reference Manual.* The Netherlands: PLAXIS bv.

Commission on Slope Stability (1995): *Anvisningar för släntstabilitetsutredningar.* Linköping: Roland Offset.

Coulomb, C. A. (1773): Essai sur une application des règles de maximis et minimis à quelques problèmes de statique relatifs à l'architecture. *7*, 343-387.

Dorf, R. C. (1996): *The Engineering Handbook.* Florida: CRC Press, Inc.

Duncan, J. M., Wright, S. G., & Brandon, T. L. (2014): *Soil Strength and Slope Stability* (Second ed.). New Jersey: John Wiley & Sons, Inc.

Edmark, C., & Hansson, A. (2011a): Beräkningshandling. *Tennet 2 - Temporära spontkonstruktioner*. Göteborg: Skanska Sverige AB.

Edmark, C., Hansson, A., & Kollberg, L. (2011b, 04 29): Bygghandling. *KV. Tennet - Temporär spont, föreskrifter och arbetsordning*. Göteborg: Skanska Sverige AB.

GOOGLE MAPS. (2017): *Map of the location of the Tennet 2 building.* Retrieved 05 15, 2017, from Google: https://www.google.se/maps/place/Tennet/@57.7143328,11.9708088,598m/data=!3m1!1e3!4m5!3m4!1s0x464ff49d864f364d:0x5a20254113e6e765!8m2!3d57.71433!4d11.9729975

Hansson, A. (2011a, 03 10): Markteknisk undersökningsrapport/Geoteknik. *Tennet 2 Gullbergsvass 5:24, Göteborgs Stad*. Göteborg: Skanska Sverige AB.

Hansson, A. (2011b, 04 13): Projekterings-PM, Geoteknik. *Tennet 2 Gullbergsvass 5:24, Göteborgs stad*. Göteborg: Skanska Sverige AB.

Hutton, J. (1795): *Theory of the earth: With proofs and illustrations* (Vol. 1). Library of Alexandria.

Ismail, A., & Teshome, F. (2011): *Analysis of deformations in soft clay due to unloading.* Master's Thesis. Department of Civil and Environmental Engineering. Gothenburg: Chalmers University of Technology.

Karlsrud, K., & Andresen, L. (2005): Loads on braced excavations in soft clay. *International Journal of Geomechanics, 5*(2), 107-113.

Karstunen, M. (2016): *Lecture N1: Introduction to numerical modelling & finite elements in the course BMT041 Infrastructural Geo-Engineering.* Chalmers University of Technology, Göteborg.

Knappett, J. A., & Craig, R. F. (2012): *Craig's soil mechanics* (Eight ed.). Abingdon: Spon Press.

Kullingsjö, A. (2007): *Effects of deep excavations in soft clay on the immediate sourroundings-Analysis of the possibility to predict deformations and reactions against the retaining system.* Ph.D Thesis. Department of Civil and Environmental Engineering. Gothenburg: Chalmers University of Technology.

Kullingsjö, A. (2011a): Inklinometrar. *[Excel File]*. Göteborg: Skanska Sverige AB.

Kullingsjö, A. (2011b): Kontrollprogram mätvärden AK. *[Excel File]*. Göteborg: Skanska Sverige AB.

Kullingsjö, A. (2011c): Tennet 2 2D-beräkning. *[PLAXIS 2D File]*. Skanska Teknik, Göteborg.

Labuz, J. F., & Zang, A. (2012): *Mohr-Coulomb Failure Criterion.* Minneapolis: University of Minnesota.

Neher, H. P., & Wehnert, M. (2001): An evaluation of soft soil models based on trial embankments. In C. S. Desai, T. Kundu, S. Harpalani, & J. Kemeny, *In Computer Methods and Advances in Geomechanics: Proceedings of the 10th International Conference on Computer Methods and Advances in Geomechanics* (p. 373). Arizona: CRC Press.

Orr, T. L., & Farrell, E. R. (2012): *Geotechnical Design to Eurocode 7.* Dublin: Springer Science & Business Media.

Persson, J. (2004): *The unloading modulus of soft clay: A field and laboratory study.* Licentiate Thesis. Department of Geo Engineering. Gothenburg: Chalmers University of Technology.

Puzrin, A. M., Alonso, E. E., & Pinyol, N. M. (2010): *Geomechanics of Failures.* Springer Science & Business Media.

Rankine , W. J. (1857): *On the stability of loose earth.* London: Philosophical Transactions of the Royal Society of London.

Ryner, A., Fredriksson, A., & Stille, H. (1996): *Sponthandboken: handbok för konstruktion och utformning av sponter.* Stockholm: Byggforskningsrådet.

Smoltczyk, U. (. (2002): *Geotechnical Engineering Handbook, Fundamentals* (Vol. 1). Berlin: Ernst & Sohn.

Sällfors, G. (2009): *Geoteknik: jordmateriallära - jordmekanik* (Fourth ed.). Göteborg: Chalmers tekniska högskola.

Terzaghi, K. (1925): *Erdbaumechanik auf bodenphysikalischer Grundlage.* Liepzig-Vienna: Franz Deuticke.

Appendices

Appendix A – Blueprints of Tennet 2

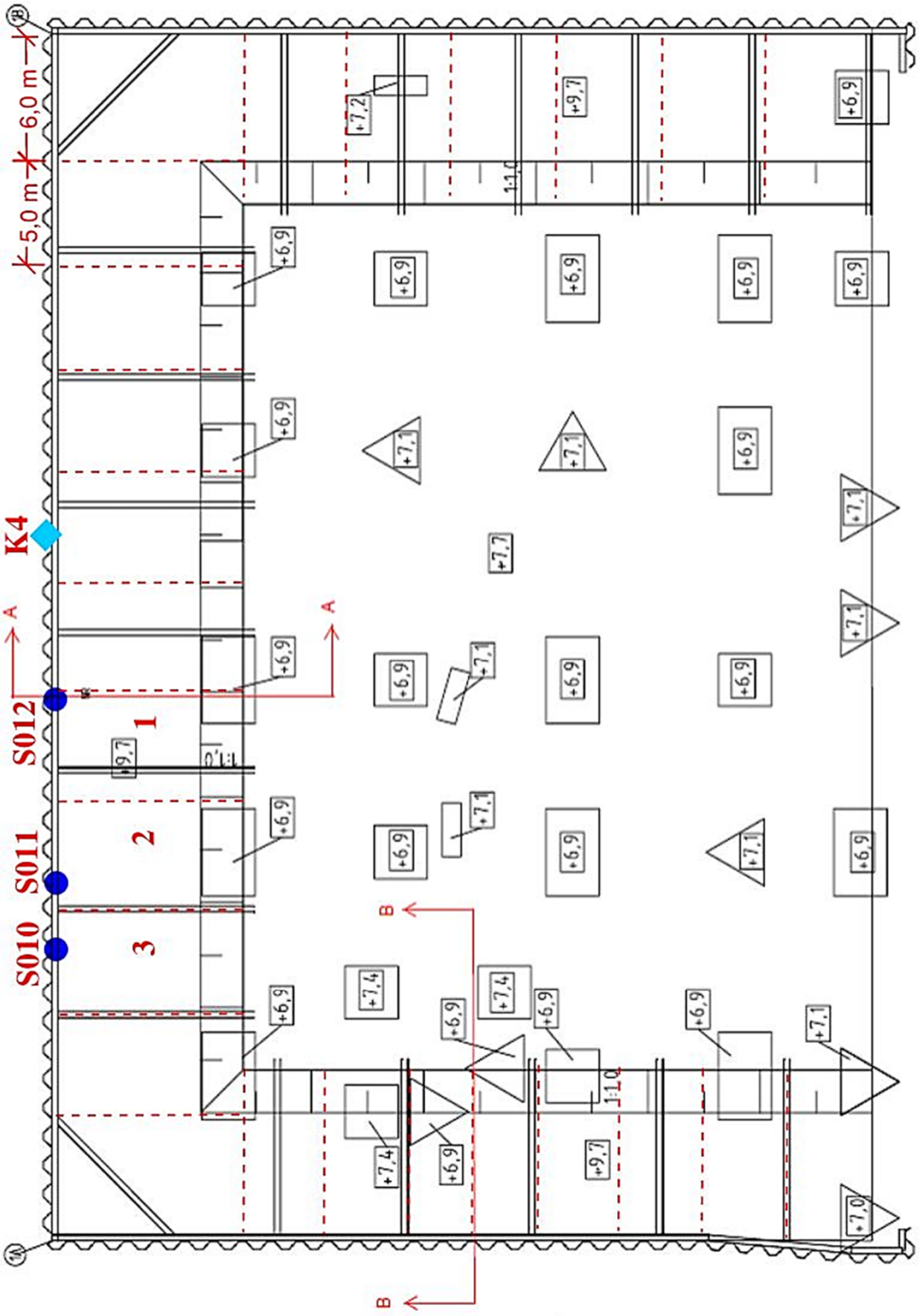

Figure A.1 *Locations of the nodes S010, S011 and S012, and inclinometer K4. 1, 2 and 3 represent the three excavation stages (modified blueprints of Tennet 2).*

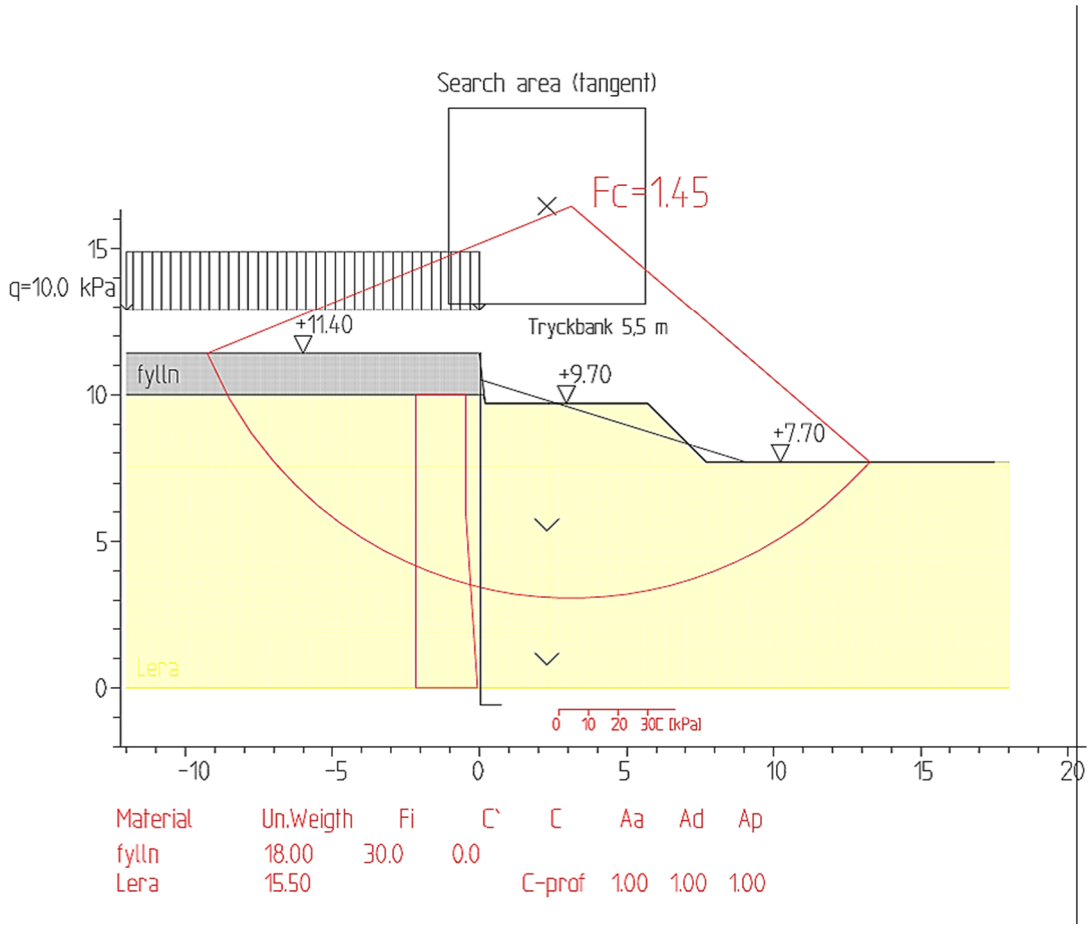

Figure A.2 Resulting factor of safety, Fc (Edmark & Hansson, 2011a).

Appendix B – Hand-calculations of earth pressures

Table B.1 Input parameters for the soil.

	Fill	Clay 1	Clay 2	Clay 3	Clay 4
Level	+11,5 / +9,7	+9,7 / +6,0	+6,0 / +0,0	+0,0 / -13,0	-13,0 / -20,0
Material behaviour	Drained	Undrained	Undrained	Undrained	Undrained
γ [kN/m^3]	21	15,5	16	16,5	16,5
c_u [kN/m^2]	-	17	17	21	37
c' [kN/m^2]	1	-	-	-	-
φ' [°]	30	-	-	-	-
K_a [-]	0,33	-	-	-	-
K_p [-]	3	-	-	-	-

Table B.2 Necessary lengths for the calculations.

Length wall [m]	12
Depth excavation [m]	3,8
Depth Head [m]	1,4

Table B.3 Lateral earth pressures calculated by hand.

Depth [m]	Active [kPa]	Passive [kPa]	Net pressure [kPa]
11,5	0,0	0,0	0,0
10,1	-7,2	0,0	-7,2
9,7	-12,7	0,0	-12,7
7,7	-26,6	34,0	-26,6 / 7,4
6,0	-53,0	65,0	12,1
0,0	-149,0	156,4	7,4
-0,5	-149,2	172,6	23,4

Appendix C – Constant Rate of Strain tests

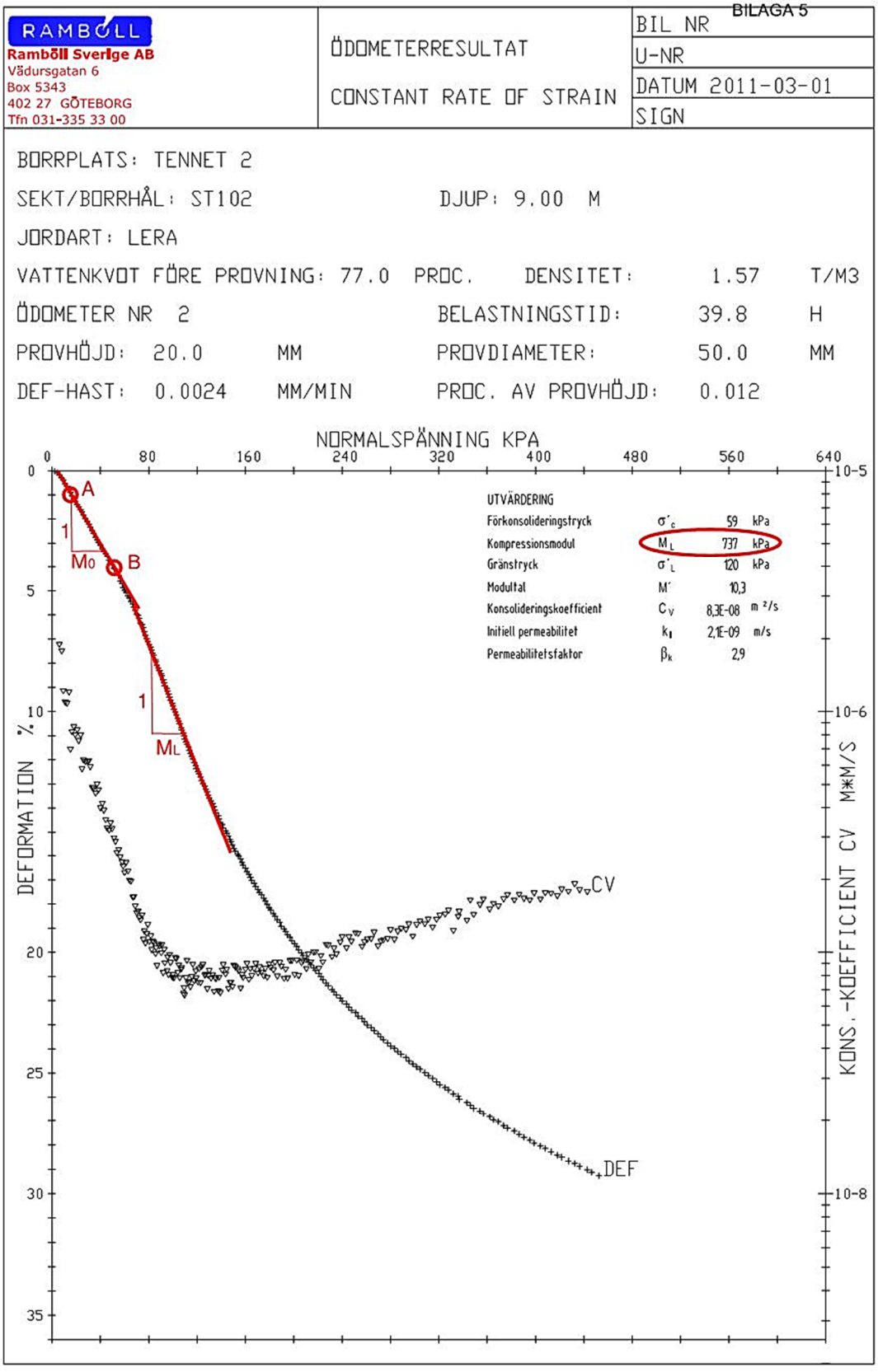

Figure C.1 Constant Rate of Strain test at the depth of 9 meter (Hansson, 2011a [modified]).

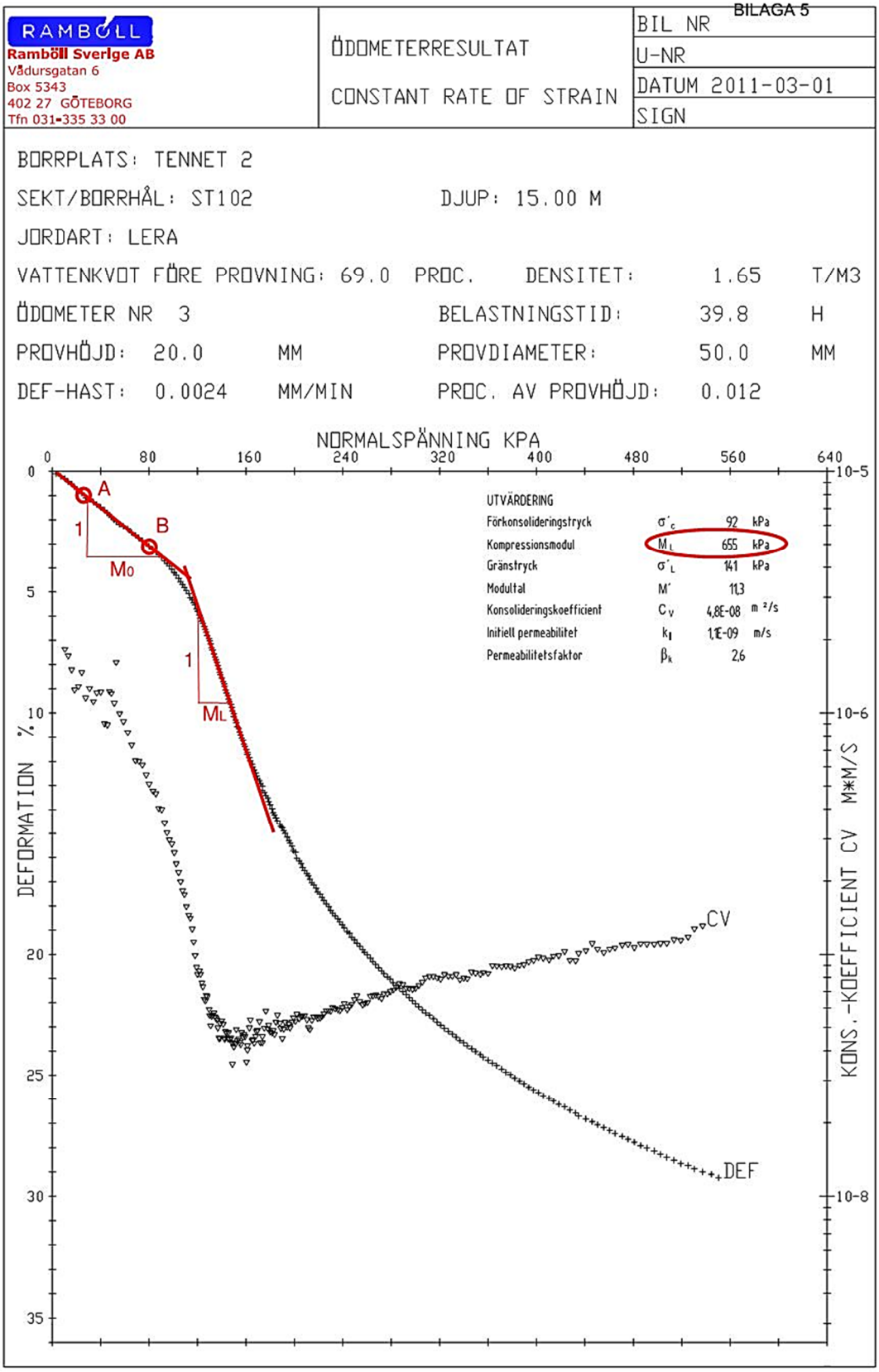

Figure C.2 Constant Rate of Strain test at the depth of 15 meter (Hansson, 2011a [modified]).

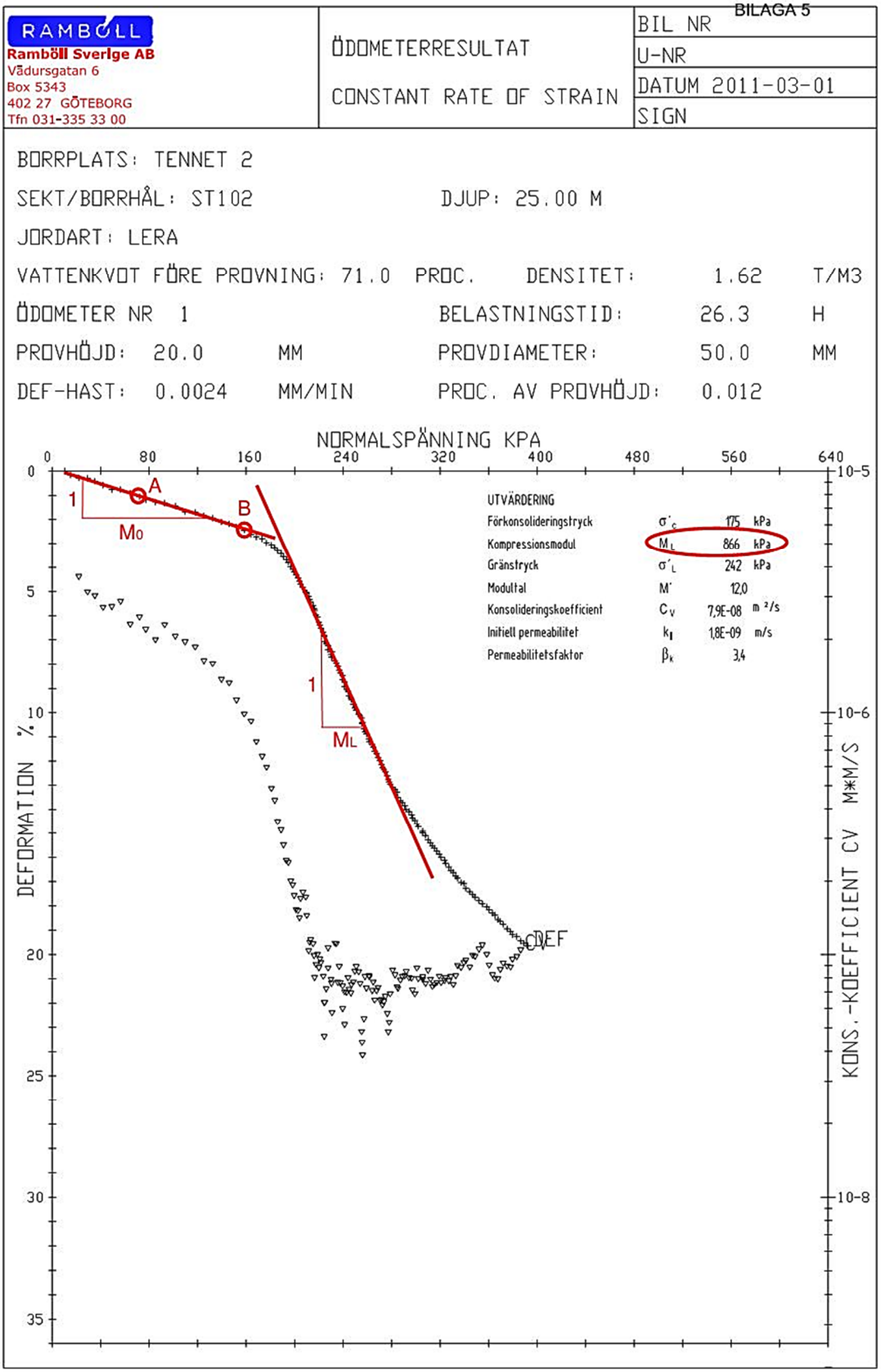

Figure C.3 Constant Rate of Strain test at the depth of 25 meter (Hansson, 2011a [modified]).

Appendix D – Deriving of soil parameters for the Soft Soil model

By evaluating the CRS-tests in Appendix C, the values of λ^* and κ^* were calculated by using equations D.1 and D.2

$$\lambda^* \approx \frac{1.1 \cdot \sigma'_{vc}}{M_L} \tag{D.1}$$

$$\kappa^* \approx \frac{2 \cdot \sigma'_v}{M_{ur}} \tag{D.2}$$

σ'_{vc} denotes the average between the preconsolidation stress, σ'_c, and the defined stress, σ'. σ'_v is the average stress in the range before the preconsoidation stress. M_L is the compression modulus for the virgin compression line and M_{ur} is the compression modulus for the unloading/reloading compression line. Since there were no unloading/reloading compression lines in the tests, the value of M_{ur} could be estimated by evaluating M_0, which is the compression modulus before the preconsolidation pressure. M_{ur} could be calculated as 3 to 6 times the value of M_0, hence $M_{ur,1}$ and $M_{ur,2}$ in Table D.1. M_0 was calculated by using equation D.3

$$M_0 = \frac{\varepsilon_B - \varepsilon_A}{\sigma_B - \sigma_A} \tag{D.3}$$

The compiled data from the CRS-tests along with calculated parameters are presented in Table D.1.

Parameter	**Unit**	**CRS-test**		
		9m	**15m**	**25m**
M_L	[kPa]	737	655	866
σ'_c	[kPa]	59	92	175
σ'	[kPa]	69.75	107.5	172.5
σ'_{vc}	[kPa]	64.38	99.75	173.75
σ'_v	[kPa]	34.5	51	95
λ^*	[-]	0.096	0.168	0.221
M_0	[kPa]	1093.75	2272.73	5625
$M_{ur,1}$	[kPa]	3281.25	6818.18	16875
κ_1^*	[-]	0.021	0.0145	0.011
$M_{ur,2}$	[kPa]	6562.5	13636.36	33750
κ_2^*	[-]	0.011	0.007	0.006

Appendix E – Validation of the sheet pile wall length

As can be seen in Figure 5.4 and 5.5 in Chapter 5.2.1, the net pressures were close to zero kPa below the bottom of the excavation and the wall appeared to be overdimensioned. In order to validate the length of the sheet pile wall, back-calculation of the factor of safety was performed. As can be seen in Figure A.2 in Appendix A, the retrieved factor of safety when dimensioning the sheet pile wall at the time of the Tennet 2 project, was 1.45. Therefore, an additional phase was added after the last phase in the PLAXIS 2D calculations, including the Mohr-Coulomb model with drainage type Undrained (B). This phase was set to iterate reduction of the friction angle and undrained shear strength in the soil, until the factor of safety was reduced to 1.45. The resulting lateral earth pressures can be seen in Figure E.1, where the red arrows represent the forces from the wailing beam and the coarse concrete. Clear similarities can be seen when comparing it to the earth pressures calculated by Skanska, at the time of the Tennet 2 project, see Figure E.2.

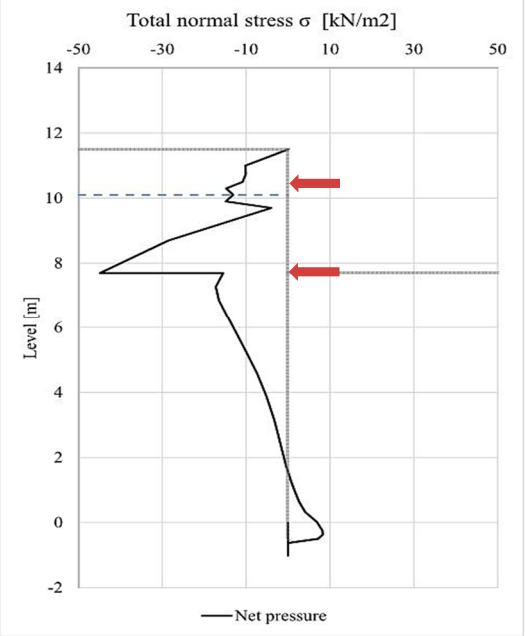

Figure E.1 *Calculated lateral earth pressure with the Mohr-Coulomb model plastic Undrained (B), safety factor 1.45.*

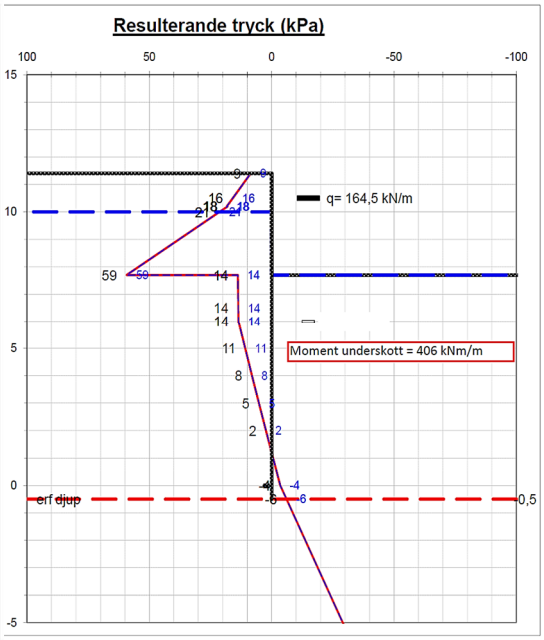

Figure E.2 *Calculated lateral earth pressure during the design of the Tennet 2 project (Edmark & Hansson, 2011a).*